Bull Volcanol (2007) 70:23–54
DOI 10.1007/s00445-007-0118-5

RESEARCH ARTICLE

Incursion of a large-volume, spatter-bearing pyroclastic density current into a caldera lake: Pavey Ark ignimbrite, Scafell caldera, England

Peter Kokelaar · Pamela Raine · Michael J. Branney

Received: 16 January 2004 / Accepted: 19 November 2006 / Published online: 17 March 2007

Abstract The Scafell caldera-lake volcaniclastic succession is exceptionally well exposed. At the eastern margin of the caldera, a large andesitic explosive eruption (>5 km^3) generated a high-mass-flux pyroclastic density current that flowed into the caldera lake for several hours and deposited the extensive Pavey Ark ignimbrite. The ignimbrite comprises a thick (≤125 m), proximal, spatter- and scoria-rich breccia that grades laterally and upwards into massive lapilli-tuff, which, in turn, is gradationally overlain by massive and normal-graded tuff showing evidence of soft-state disruption. The subaqueous pyroclastic current carried juvenile clasts ranging from fine ash to metre-scale blocks and from dense andesite through variably vesicular scoria to pumice (<10^3 kg m^{-3}). Extreme ignimbrite lithofacies diversity resulted via particle segregation and selective deposition from the current. The lacustrine proximal ignimbrite breccia mainly comprises clast- to matrix-supported blocks and lapilli of vesicular andesite, but includes several layers rich in spatter (≤1.7 m diameter) that was emplaced in a ductile, hot state. In proximal locations, rapid deposition of the large and dense clasts caused displacement of interstitial fluid with elutriation of low-density lapilli and ash upwards, so that these particles were retained in the current and thus overpassed to medial and distal reaches. Medially, the lithofacies architecture records partial blocking, channelling and reflection of the depletive current by substantial basin-floor topography that included a lava dome and developing fault scarps. Diffuse layers reflect surging of the sustained current, and the overall normal grading reflects gradually waning flow with, finally, a transition to suspension sedimentation from an ash-choked water column. Fine to extremely fine tuff overlying the ignimbrite forms ~25% of the whole and is the water-settled equivalent of co-ignimbrite ash; its great thickness (≤55 m) formed because the suspended ash was trapped within an enclosed basin and could not drift away. The ignimbrite architecture records widespread caldera subsidence during the eruption, involving volcanotectonic faulting of the lake floor. The eruption was partly driven by explosive disruption of a groundwater-hydrothermal system adjacent to the magma reservoir.

Keywords Caldera · Explosive volcanism · Ignimbrite breccia · Lacustrine sediment · Spatter · Subaqueous density current

Editorial responsibility: J McPhie

P. Kokelaar (✉) · P. Raine
Earth and Ocean Sciences Department, University of Liverpool, Liverpool L69 3BX, UK
e-mail: p.kokelaar@liv.ac.uk

M. J. Branney
Geology Department, University of Leicester, Leicester LE1 7RH, UK

Present address:
P. Raine
ExxonMobil Exploration Company, P.O. Box 4778, Houston, TX 77210, USA

Introduction

Most large-scale explosive eruptions at caldera volcanoes are interpreted from pyroclastic deposits that are exposed at caldera walls and on outer volcano flanks. The most proximal deposits seen typically include ignimbrite deposited from high-mass-flux pyroclastic currents. Many proximal ignimbrites are dominated by coarse breccias that show dramatic thickening into topographic lows, clast-imbrication, dune forms, and gradations into ash- and pumice-rich ignimbrite (e.g. Druitt and Sparks 1982; Druitt and Bacon

1986). It is reasonable to expect that proximal ignimbrite also occurs within the caldera, but little is known about such deposits, because they are mostly concealed at modern caldera volcanoes. The rare opportunity to study the caldera-lake deposit of a large explosive eruption is presented by the Ordovician Scafell caldera volcano in the English Lake District (Fig. 1), where the 300–540 m-thick caldera-lake succession has been deeply dissected by glaciers in mountainous terrain, providing excellent continuity of exposure (Branney and Kokelaar 1994; Raine 1998).

Proximal ignimbrite breccias are typically clast-supported and, locally, open-work and fines-poor. It is generally inferred that originally abundant ash in the parent current was vigorously elutriated away from the proximal sites of deposition and carried more distally, because most proximal ignimbrite breccias grade laterally or distally into ash-rich ignimbrite lithofacies (e.g. Druitt et al. 1989; Branney and Kokelaar 2002). Some proximal ignimbrite breccias are predominantly composed of lithic clasts, others are predominantly composed of juvenile clasts ranging from dense spatter to vesicular scoria, and some examples comprise variable mixtures of lithic and juvenile fragments (e.g. Marsella et al. 1987; Druitt et al. 1989; Clavero and Moreno 1994; Perrotta and Scarpati 1994; Robin et al. 1994; Rosi et al. 1996; Branney and Kokelaar 2002). Pancake and amoeboid forms of large juvenile fragments indicate ductile behaviour during emplacement (Mellors and Sparks 1991; Allen 2005); agglutination can accompany deposition to form welded scoria or spatter agglomerate (Wright and Walker 1981; Druitt et al. 1989; Palladino and Simei 2004). In many deposits the juvenile clasts show evidence of pre- or syn-eruptive admixture of small lithic fragments, as well as surface chilling and cracking during brief exposure to water before deposition. Proximal ignimbrite breccias that contain abundant fluidal-shaped juvenile fragments are commonly associated with flooded calderas (e.g. Campi Flegrei, Latera, Santorini, Taal and Villarica; references above) and many show evidence of emplacement during climactic eruption phases that involved caldera collapse. The eruption of the dense juvenile clasts may reflect catastrophic disruption of a hydrothermal system adjacent to a depressurising magma chamber, or beneath a lava lake, with explosive expansion of water providing the means for driving out the relatively gas-poor magma (e.g. Mellors and Sparks 1991; Druitt et al.

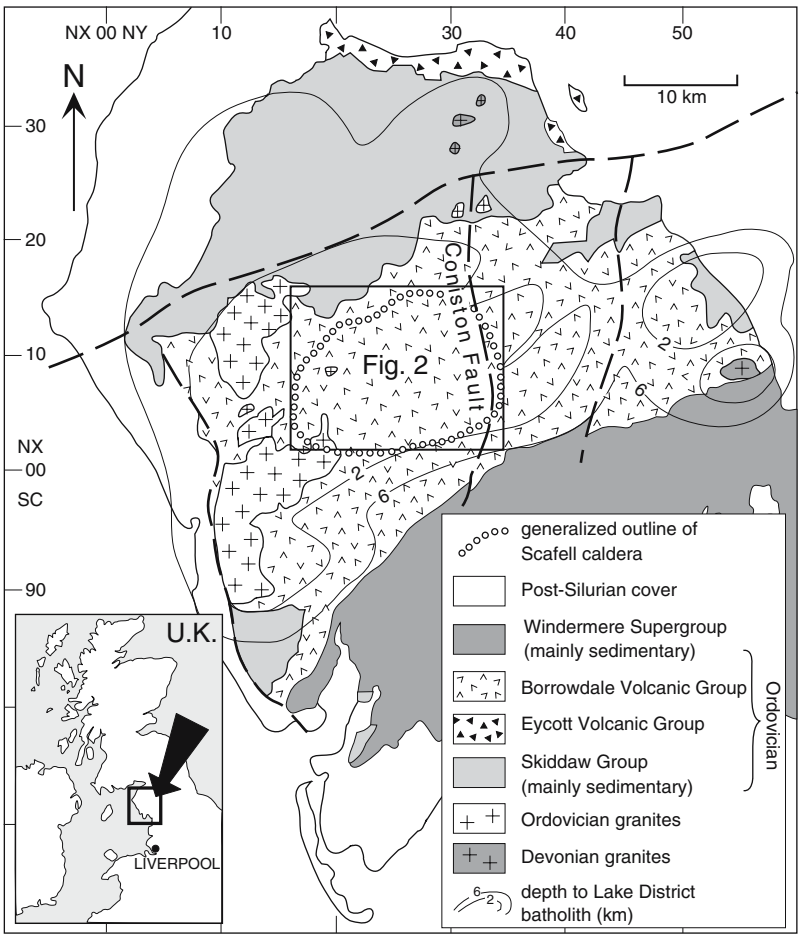

Fig. 1 Geological map of the English Lake District showing the Ordovician Borrowdale Volcanic Group, with underlying Ordovician Skiddaw Group sedimentary strata and overlying Ordovician–Silurian Windermere Supergroup sedimentary strata; *inset* shows location in UK. The study area is shown by the *box* labelled Fig. 2. Map coordinates are from the UK Ordnance Survey National Grid

1989). However, such phreatomagmatic activity is not fully understood; caldera volcanoes probably all have hydrothermal systems at depth and the possible influence of any overlying body of standing water, especially during caldera collapse, is not known. Similar deposits also occur in settings that apparently lacked substantial standing water in the vent area, for example at Summer Coon (Valentine et al. 2000), Tambora (discussion in Mellors and Sparks 1991), and Tanna (Allen 2005).

We provide the first account of a thick proximal ignimbrite breccia and laterally correlative ash-rich ignimbrite lithofacies that were emplaced in a caldera lake with accompanying caldera subsidence. The deposit records what happens during sustained flow of a large pyroclastic density current beneath water; although much of the current mixed with the water, some basal parts in proximal areas evidently had no direct contact with liquid water and remained gaseous. From the relatively few detailed accounts of deposits of subaqueous pyroclastic density currents, it seems that current types range from those that are of sufficiently high mass-flux so that they retain gaseous interstitial fluid in parts and hot-state (>100°C) deposition can occur proximally (Sigurdsson et al. 1991; Mandeville et al. 1996), sometimes involving subaqueous welding (Kokelaar and Busby 1992; Kokelaar and Königer 2000), through to types that have thoroughly mixed with water, contain little or no gas, and form deposits with little heat retention (Fiske 1963; Fiske and Matsuda 1964; Carey and Sigurdsson 1980; Wright and Mutti 1981; Whitham 1989; Cole and DeCelles 1991). We infer that the Pavey Ark current was of the former type.

The Pavey Arc deposit also illustrates how a catastrophic subaqueous current interacts with basin-floor topography; correlated layers constitute time-surfaces that allow the aggradation history to be reconstructed ('entrachrons' of Branney and Kokelaar 2002), and they show that volcano-tectonic subsidence was occurring while the ignimbrite was being emplaced. Finally, entrapment of the current within a caldera lake allows estimation of the entire grain-size population of the current; this is in contrast to subaerial pyroclastic density currents and unconfined turbidity currents (e.g. subaqueous currents from the Roseau eruption; Whitham 1989), from which much of the fines population is elutriated and lofted or dispersed down-current so that a true picture of the transported load is obscured.

Terminology

We use primary volcaniclastic terminology (e.g. breccia, lapilli-tuff, ignimbrite, co-ignimbrite ash or tuff) for the Pavey Ark deposit, because we infer that it was emplaced directly from a primary pyroclastic current, without any temporary storage or sedimentary reworking (cf. White and Houghton 2006). The density current originated from a large, sustained explosive eruption of gas, variably vesicular juvenile clasts including scoria and pumice, and abundant ash. Hence we refer to the deposit as ignimbrite, although, importantly, we do not imply by this that the entire current was gas-charged. Medial to distal and upper parts of the current were aqueous dispersions containing little or no gas; all the lithofacies transitions are intergradational and relate to a single syn-eruptive event. We have found no lithofacies transition that clearly marks a change of interstitial fluid from gas to liquid, but such a transition need not be expected, because a change of fluid need not occur abruptly (parts of the current may have been a three-phase slurry of liquid, gas and particles) and because the sedimentation behaviour of poorly sorted, high-concentration (low voidage) dispersions may not differ greatly with either water or (compressed) dusty gas as interstitial fluids. We use 'ignimbrite' to include all lithofacies produced directly from the primary pyroclastic current, and, similarly, we use co-ignimbrite ash or tuff for the water-settled deposit from the wake and plume formed above the sustained primary current.

Ignimbrites generally derive from explosive eruptions of particulate dispersions that initially have a bulk density probably little more than an order of magnitude greater than the atmosphere at sea-level (1.25 kg m^{-3}), and significantly less than water (~10^3 kg m^{-3}) (e.g. Sparks et al. 1997). However, most pyroclastic density currents will develop pronounced density stratification (e.g. Valentine 1987; Burgisser and Bergantz 2002) and this stratification is a prerequisite for part of a current to flow under water as a coherent entity. We refer to particulate density currents with a high-concentration lowermost part as *granular-fluid-based currents* (Branney and Kokelaar 2002); this term makes no statement about the concentration and flow behaviour of parts of the current above the lowermost part. In granular-fluid-based currents, particle support near the lower flow boundary is dominated by grain interactions and upward displacement of interstitial fluid by depositing clasts (sedimentation–fluidization). Such currents range from those in which almost the entire thickness is composed of a granular fluid (e.g. a fully shearing granular flow) to mainly dilute turbulent flows with high concentration only near the lower flow boundary. In *fully dilute currents*, particle support is primarily due to fluid turbulence right down to the base (Branney and Kokelaar 2002). Fully dilute pyroclastic density currents would not be dense enough to enter standing water.

The architecture of lithofacies within an ignimbrite records aspects of the temporal and spatial evolution of a pyroclastic current. The lithofacies reflect processes and conditions in the lower flow-boundary zone of the current during deposition. Vertical variations in lithofacies record flow-boundary zone unsteadiness, whereas lateral variations record non-uniformity. Deposit thickness depends on sedi-

mentation rate and duration. Grain-size distributions and components of single lithofacies are unlike the bulk population of the parent current; sorting characteristics of the deposit reflect both clast attrition and clast segregation during transport and deposition.

In this paper we (1) establish that the Pavey Ark ignimbrite and co-ignimbrite ash were emplaced beneath water, (2) document the various lithofacies and interpret their depositional processes, (3) describe and interpret the three-dimensional lithofacies architecture, including features that resulted from pre-existing lake-floor topography and from syn-eruptive caldera subsidence, and (4) discuss the nature of the explosive eruption, making comparisons with other caldera-collapse related eruptions elsewhere. We present an empirical model in which a single, sustained, high-mass-flux pyroclastic density current produces an extremely diverse range of lithofacies within a confined basin.

Scafell caldera volcano

Scafell caldera volcano (Figs. 1 and 2; Branney and Kokelaar 1994) lies within a 6 km-thick succession of predominantly subaerial calc-alkaline lavas, pyroclastic rocks, volcanogenic sedimentary rocks and high-level intrusions, which together comprise the Ordovician (Caradoc) Borrowdale Volcanic Group (Millward 2002). The volcano is one of several nested centres preserved by caldera collapse and extension-related subsidence within a continental arc (Branney 1988; Branney and Soper 1988). It overlies a coeval batholith (Fig. 1), which has substantially protected it from tectonic shortening (Acadian orogeny; Soper et al. 1987), and the rocks have been affected by low-grade regional metamorphism and locally pervasive hydrothermal alteration.

Scafell caldera, ~17×14 km (Fig. 2), formed during several explosive eruptions involving tens to hundreds of km^3 of andesitic to rhyolitic magma and emplacement of a succession of ignimbrites (Whorneyside and Airy's Bridge Formations; Fig. 3). The intracaldera ignimbrites and associated mesobreccias reveal a complex pattern of caldera-floor fragmentation and differential subsidence along numerous intersecting faults; downsag (inward-tilting) during this piecemeal collapse is evident from thickness variations of the ignimbrites (Branney and Kokelaar 1994) and from palaeomagnetic studies (Channell and McCabe 1992; Piper et al. 1997). Caldera collapse was followed by deposition of talus breccias along active and degrading fault scarps, and by subaerial extrusion of two lava domes: Scafell Dacite and Rosthwaite Rhyolite (Figs. 2 and 3). The Scafell Dacite lava dome formed a substantial topographic feature within the caldera, extending laterally for over 4 km with an average thickness of ~90 m and a summit more than 425 m above its base (Kneller et al. 1993).

Scafell caldera-lake succession

Soon after extrusion of the lava domes, a lake formed in Scafell caldera and subaqueous deposition of pyroclastic and volcanogenic sediments began; these strata constitute the Seathwaite Fell Formation (Kneller and McConnell 1993; Raine 1998; Figs. 2 and 3). A freshwater lake rather than a marine basin is indicated by the absence of body and trace fossils, and by the lack of any marine lithofacies or non-volcanic detritus, although some temporary connection with the sea (e.g. as at Taal caldera, Philippines) cannot be ruled out. A minimum size of the lake is defined by the 100 km^2 extent of the lacustrine succession (Fig. 2), but it was probably considerably larger than this; the sedimentary deposits exhibit no evidence of significant wave reworking or shorelines and the structural limits of Scafell caldera indicate an area of at least 190 km^2. However, the caldera margins were broad and complex, with inward-tilted strata and extensive gentle slopes, rather than steeply walled, and the lake size probably changed with time. The only evidence of shallowing and emergence is at the top of the succession. Reactivation of caldera-floor faults occurred after flooding; seismic shock caused locally intense soft-sediment disruption, and the Troughton Beck and Blea Tarn faults (Fig. 2) produced lake-floor topography that influenced sediment pathways during caldera-lake sedimentation (Kneller and McConnell 1993). The eventual demise of the lake is marked by subaerially emplaced tuff-ring and ash-fall deposits towards the top of the Seathwaite Fell Formation (Brown 2001), and thick ignimbrites (Lincomb Tarns Formation; McConnell 1993; Figs. 2 and 3).

The caldera-lake succession records deposition of mainly fine-grained volcanogenic sediment, punctuated by abrupt incursions of coarse-grained volcanic debris (Fig. 4). Sedimentary terminology is used uniformly to describe the non-Pavey Ark silt- and sand-grade deposits (e.g. fine sandstone as opposed to fine tuff; Fig. 5), because mostly we are unable to discriminate between fine-grained deposits due to primary volcanic dispersal and those due to secondary dispersal (reworking). The massive to faintly laminated siltstone beds are interpreted as representing settling of ash that either fell into the lake or was suspended from hyperpycnal flows, interflows or turbidity currents. Normal-graded sandstone beds with massive, parallel and cross-laminated divisions are interpreted as turbidites. Very poorly sorted pebbly sandstones are interpreted as deposits of high-density turbidity currents and debris flows. Several such layers contain diagenetically flattened pumice clasts

Fig. 2 Simplified geological map of Scafell caldera volcano in the Central Fells of the English Lake District. Numerous minor intrusions and faults have been omitted for clarity. Map coordinates relate to Ordnance Survey National Grid Square NY ▶

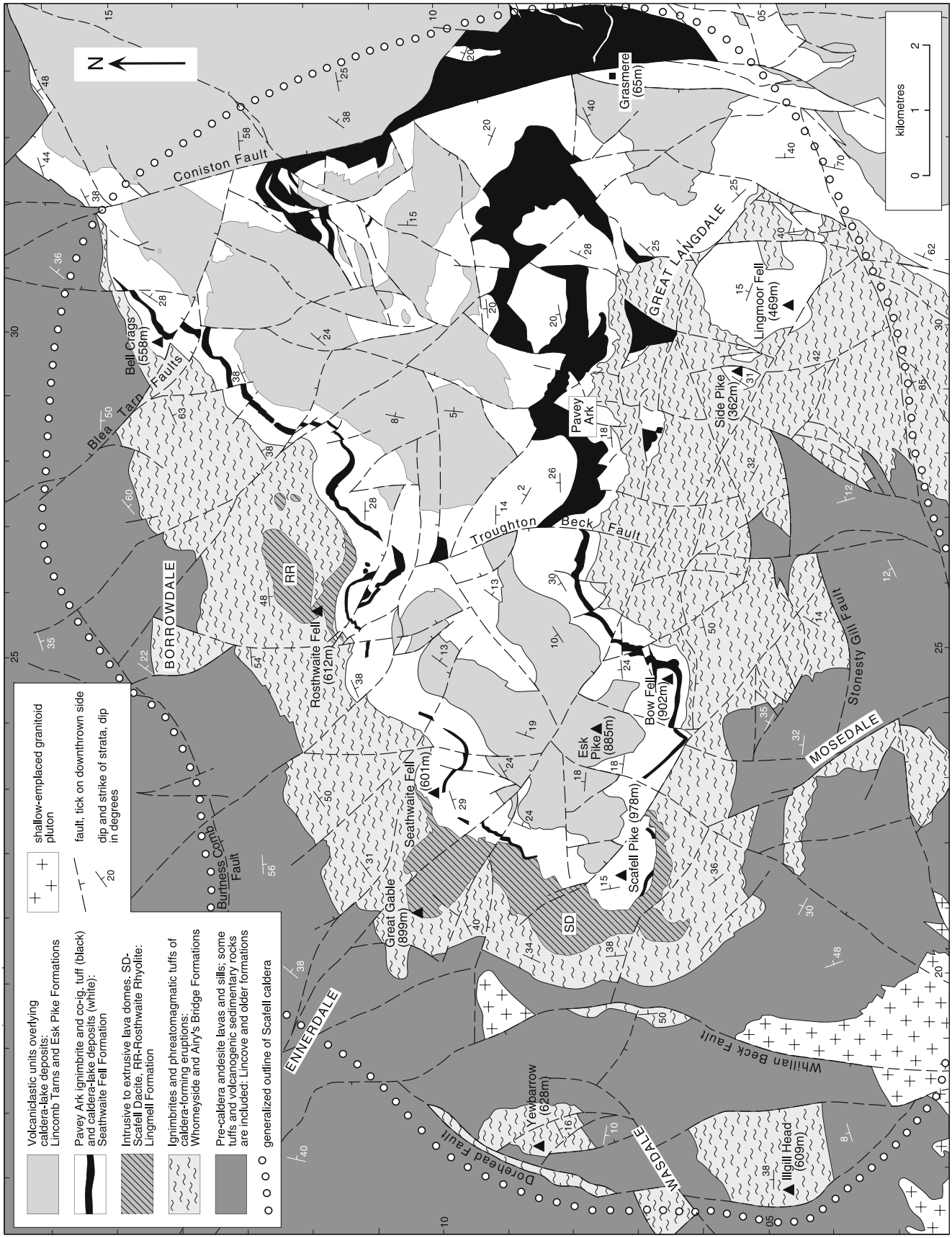
Volcaniclastic units overlying caldera-lake deposits: Lincomb Tarns and Esk Pike Formations
Pavey Ark ignimbrite and co-ig. tuff (black) and caldera-lake deposits (white): Seathwaite Fell Formation
Intrusive to extrusive lava domes. SD-Scafell Dacite, RR-Rosthwaite Rhyolite: Lingmell Formation
Ignimbrites and phreatomagmatic tuffs of caldera-forming eruptions: Whorneyside and Airy's Bridge Formations
Pre-caldera andesite lavas and sills; some tuffs and volcanogenic sedimentary rocks are included: Lincove and older formations
generalized outline of Scafell caldera
shallow-emplaced granitoid pluton
fault, tick on downthrown side
dip and strike of strata, dip in degrees
N
kilometres
0
1
2
Coniston Fault
Blea Tarn Faults
Bell Crags (558m)
BORROWDALE
Burtness Comb Fault
Rosthwaite Fell (612m)
RR
Seathwaite Fell (601m)
Great Gable (899m)
SD
Scafell Pike (978m)
Esk Pike (885m)
Bow Fell (902m)
Troughton Beck Fault
Pavey Ark
GREAT LANGDALE
Grasmere (65m)
Lingmoor Fell (469m)
Side Pike (362m)
Stonesty Gill Fault
MOSEDALE
Whillan Beck Fault
Dorehead Fault
Yewbarrow (628m)
WASDALE
Illgill Head (609m)
ENNERDALE

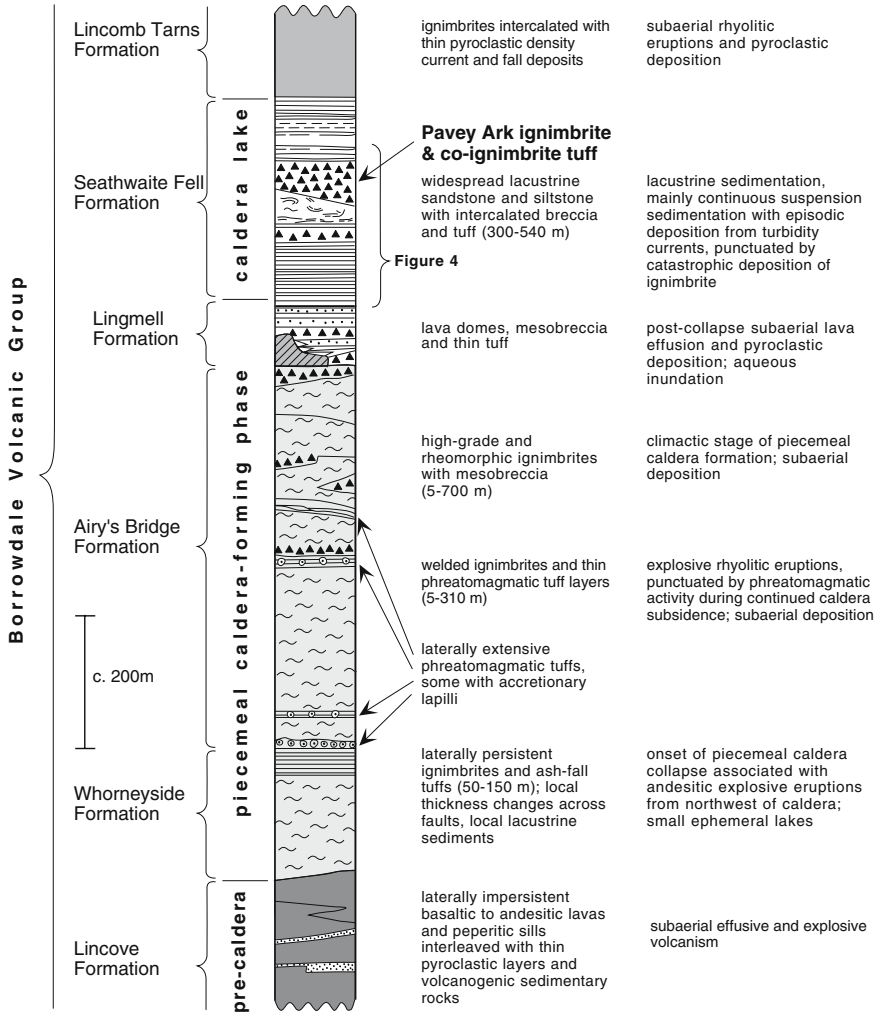

Fig. 3 Simplified stratigraphic succession of the middle part of the Borrowdale Volcanic Group exposed in the study area (Fig. 2)

(e.g. Branney and Sparks 1990) and some may be primary subaqueous counterparts of subaerial ignimbrites. The non-Pavey Ark lacustrine deposits are similar to those described from the floor of Crater Lake caldera, Oregon, where diverse origins also are inferred (Nelson et al. 1986, 1994).

Symmetrical ripples are rare, of small amplitude (≤2 cm), and occur within sequences of turbidites that also exhibit unidirectional current ripples. Given the confined nature of the basin, the ripples may result from passage of 'trains' of solitary waves (solitons) due to current reflections (e.g. Pantin and Leeder 1987; Edwards et al. 1994; Kneller et al. 1991, 1997), rather than resulting from oscillatory water motion associated with water-surface waves. Convolutions are common (Fig. 5a, b) and record both soft-state sheet sliding on basin slopes and in situ liquefaction, conceivably seismogenic in origin or due to rapid sedimentary loading.

Similarity of the lake deposits below and above the Pavey Ark unit (Fig. 4) suggests that the lacustrine sedimentary processes and environment were little altered by its emplacement, despite it being 125 m thick in places, after compaction. The implications concerning possible modification to the depth and extent of the lake water are unclear; the volume of the subaqueously emplaced Pavey Ark deposit (see below) may have been small relative to the lake volume. Given that at least 200 m of caldera-lake deposits exist above the Pavey Ark unit (Kneller and McConnell 1993), and that these deposits are broadly like the (mainly turbiditic) deposits beneath and show no sign of emergence until the top, it is reasonable to infer that the depth of water immediately before the Pavey Ark eruption could have been several hundreds of metres.

Pavey Ark ignimbrite and co-ignimbrite tuff

The andesitic Pavey Ark ignimbrite (formally the Pavey Ark Member; Kneller and McConnell 1993; British Geological Survey 1996) is named after the steep crag at its type locality (Figs. 2 and 6a; NY284 079; field locations are identified in the text by UK Ordnance Survey National Grid references

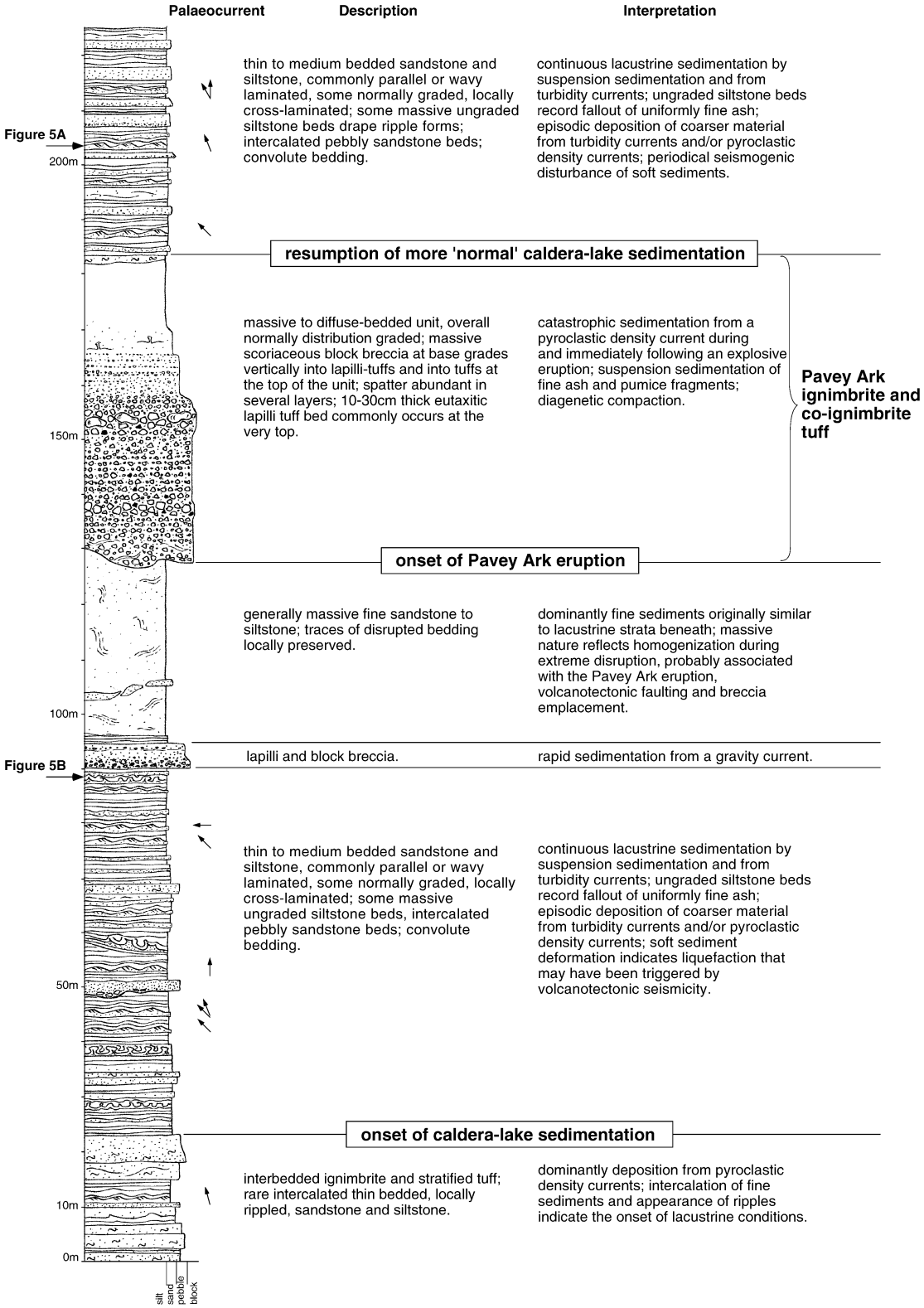

Fig. 4 Stratigraphic succession of the Seathwaite Fell Formation, based on a section logged on Bowfell (NY 2490 0602 to 2467 0652). The *log* shows the locations of photographs in Fig. 5a, b

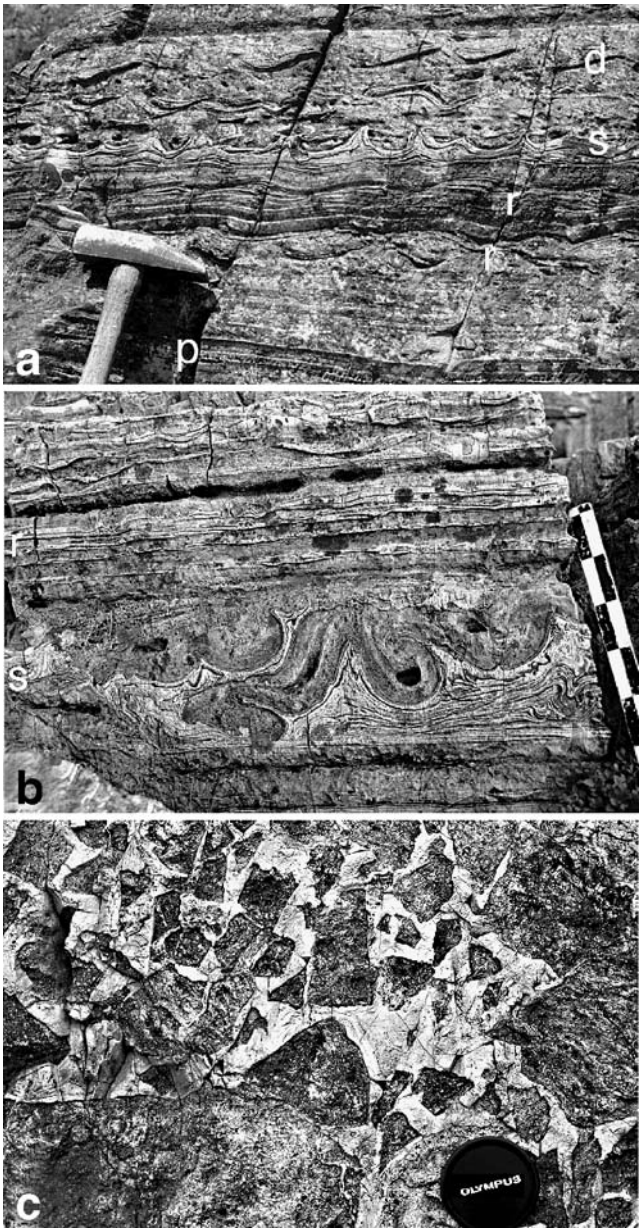

Fig. 5 Volcanogenic sediments (Seathwaite Fell Formation) deposited in Scafell caldera lake (NY 2468 0650). **a** Parallel-laminated sandstone and siltstone (*p*) overlain by asymmetric and climbing current-ripples forms (*r*), with soft-sediment load structures (*s*) and draped ripples (*d*). **b** Soft-sediment load-and-flame structure (*s*) with convolutions in bedded sandstone and laminated siltstone, indicating liquefaction due to rapid sedimentary loading and/or seismic shaking. Overlying sandstone and siltstone include starved sandstone ripples (*r*), in places draped by laminated siltstone (scale interval is 5 cm). **c** Autoclastic carapace of the subaerially emplaced Scafell Dacite lava dome with siltstone matrix formed by infiltration of lacustrine sediment (lens cap is 5 cm; NY 2130 0685)

with the prefix NY). To the north and west of Pavey Ark, the ignimbrite and its associated co-ignimbrite tuff form a well defined layer within the continuously exposed, open-folded, caldera-lake succession. This part, with a calculated volume of ~1 km^3, is the focus of the present study. East of Pavey Ark (Fig. 2), proximal ignimbrite breccia continues for 5 km and thickens to >500 m, representing at least a further 2–3 km^3. The eastern outcrops include numerous irregular andesitic intrusions and are taken to represent the source area. However, the rocks are not well exposed and are described only briefly. Farther east, and elsewhere beyond the inferred limits of the Scafell caldera, the Pavey Ark unit and possible correlatives have not yet been found. We deduce an original deposit volume in excess of 5 km^3.

The Pavey Arc ignimbrite displays striking lateral and vertical lithofacies variations, from very coarse breccia to fine tuff; it fines both upwards and westwards, and is widely overlain by very fine and extremely fine tuff. From detailed logging at 25 sites, nine main intergradational lithofacies have been recognised and are described and interpreted here (Table 1 gives a summary and volume estimates); where possible, lithofacies codes follow the scheme of Branney and Kokelaar (2002). Grain-size and abundance data have been visually estimated in the field and from thin sections. The process interpretations of each lithofacies necessarily to some extent draw from their associations, which are fully described later.

Massive breccias (mScBr; mTScBr) and agglomerate (mAg)

Description Massive scoria-rich breccia (mScBr) comprises clast-supported angular blocks and lapilli of variably scoriaceous andesite, with a sparse (≤10%) matrix of tuff (Fig. 6b, c). It is well sorted to moderately sorted; the largest clasts are typically ~15 cm in diameter, although a few larger blocks occur, mostly in the better sorted facies. Small proportions of angular lithic lapilli are virtually ubiquitous, predominantly of perlitic rhyolite. Rare angular to rounded blocks, ≤110 cm, of silicic welded ignimbrite also occur. With increasing matrix (10-15 vol.% tuff; locally up to 30 vol.%), the lithofacies is locally gradational into poorly sorted, tuffaceous scoria-rich breccia (mTScBr). The tuff matrix is commonly concentrated in layer-parallel zones, 10–40 cm thick (e.g. in the basal 20 m of log 14 of Fig. 10a), in which blocks are matrix-supported; this gives the breccia a streaky appearance. In places the breccia contains fiamme that represent original pumice fragments and impart a subtle eutaxitic fabric.

The massive breccias contain variable proportions of irregular-shaped lumps or rags of andesite, 9–170 cm in size, with smoothly curved margins, and, in some cases, folded or amoeboid forms (Fig. 7). These clasts are interpreted as spatter and where they constitute as much as 50% of the rock the lithofacies is designated as massive agglomerate (mAg; fallout origin is not implied). The spatter is sparsely vesicular, although some clasts contain a few large gas cavities, and it lacks distinct chilled or bread-crusted or

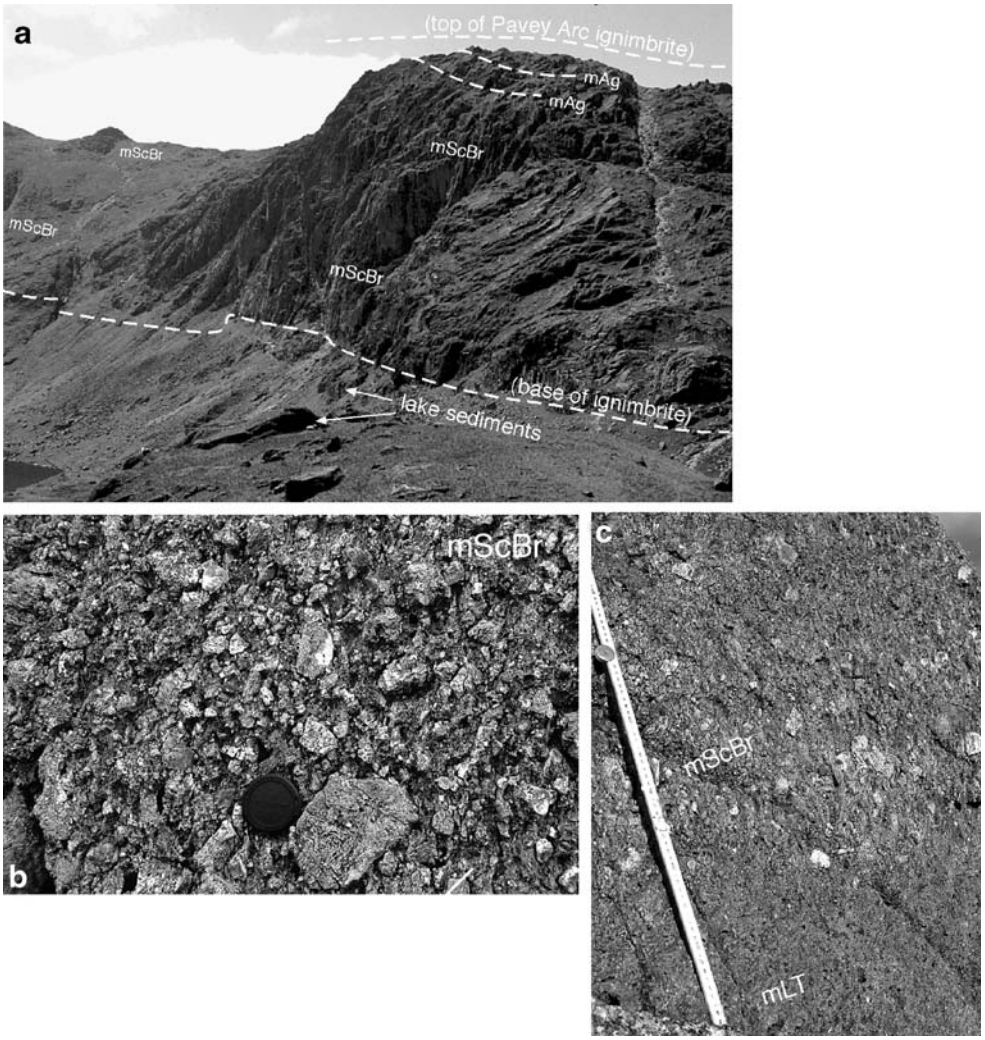

Fig. 6 Massive scoria-rich breccia (mScBr) of the Pavey Arc ignimbrite. **a** Pavey Arc (NY 284 079) viewed from the south-east, showing the 120 m-thick ignimbrite, dominated by massive scoria-rich breccia emplaced during a single eruptive event. Spatter-rich layers are indicated (mAg; Fig. 10). **b** Detail of massive scoria-rich breccia (mScBr); highly vesicular andesitic scoria forms matrix between angular blocks of andesite (NY 2839 0790). **c** Massive lapilli-tuff (mLT) grading into massive scoria-rich breccia. (Part of a metre ruler shows cm; NY 2725 1144)

cauliflower-like margins. Much of the spatter is flow-banded and some clasts are elongate (thickness-to-length ratios of about 1:7) broadly parallel to layering; imbrication has not been detected. The spatter commonly includes small lithic fragments and some clasts are wrapped around and partially enclose adjacent scoria clasts (Fig. 7b, c). Spatter occurs sparsely throughout much of massive scoriaceous breccia lithofacies (mScBr), and there are up to five layers of massive agglomerate (mAg), 1–5 m thick. Two particularly coarse layers of agglomerate (at 64–69 and 85–88 m on log 13 in Fig. 10a) contain less tuff matrix than elsewhere.

The tuff matrix comprises devitrified shards and variably vesicular, angular to cuspate scoria fragments. Curved, vesicle-wall fragments occur in breccia comprising the most vesicular scoria clasts, whereas blocky and angular shards typically occur in breccia composed of poorly vesicular scoria. Subtle gradational variations in clast sizes and sorting define vague and impersistent decimetre- to metre-scale layers. More distinct and more persistent metre-scale diffuse layers are defined by gradations into the agglomerate layers (Fig. 7a; e.g. the layer at 86 m on log 13 and at 82 m on log 14 in Fig. 10a). The breccias with agglomerates (mScBr, mTScBr and mAg) grade laterally and vertically into lapilli-tuffs (mLT, dbLT, xbLT; e.g. Fig. 6c).

Interpretation The massive breccia lithofacies are consistent with rapid progressive aggradation from a sustained, granular-fluid-based density current (Branney and Kokelaar 1992, 2002 and references therein). Absence of well developed stratification indicates deposition from a flow-boundary zone in which clast concentrations were sufficiently high to suppress turbulent segregation and development of tractional bed-forms. Massive proximal ignimbrite breccias elsewhere have also been interpreted as progressively aggraded (e.g. Walker 1985). Emplacement by en masse frictional freezing of a thick grain flow is precluded by (1) upward and down-current gradations into variably stratified lapilli-tuffs, (2) onlap relationships to lake-bed topography, and (3) thickness variations recording syn-depositional adjustment to active lake-floor volcanotectonic faulting (see

Table 1 Summary descriptions and interpretations of Pavey Ark lithofacies

Lithofacies	Description	Interpretation
mScBr Massive scoria-rich breccia	*Lithology*: Breccia of dominantly angular blocks and lapilli of dense to scoriaceous plagioclase-phyric andesite with a sparse tuff matrix; well to moderately sorted, clast-supported. Includes spatter, rare lithic blocks and ubiquitous lithic lapilli, including perlitic rhyolite and ignimbrite. *Structure*: Massive. Non-graded to graded with slight variations in clast size and type. Eutaxitic texture in places. *Occurrence*: Volume ~0.2 km^3 (~20% of lacustrine deposit). Forms basal thick accumulation; grades downcurrent and up into mTScBr and also into mAg, mLT, dbLT and xbLT.	Rapid deposition from a granular-fluid-based pyroclastic density current. Massive nature indicates that basal turbulence and traction were suppressed by high basal concentrations. Sorting strongly affected by proximal deposition of blocks and elutriation of fines by fluid displaced during rapid block settling; segregation enhanced by overpassing. Grading indicates subtle unsteadiness during sustained deposition.
mTScBr Massive tuffaceous scoria-rich breccia	*Lithology*: Breccia as above (mScBr), but with a higher proportion (10–30%) of fine ash matrix, so moderately to poorly sorted. *Structure*: Ash matrix concentrated in layer-parallel patches (10–40 cm thick) gives the breccia a streaky texture. Locally eutaxitic. *Occurrence*: Volume ~0.2 km^3 (~20%); grades variably into the massive scoria-rich breccia (mScBr).	Same as for the mScBr (above) but higher proportions of fine ash matrix primarily reflect less efficient elutriation and overpassing, partly reflecting smaller size of largest blocks deposited.
mAg Massive spatter-agglomerate	*Lithology:* Scoria-rich breccia (as above) with ≥50 vol.% spatter rags (<170 cm) with fluidal (folded, amoeboid) shapes. Spatter rags contain small lithic clasts. *Structure*: Massive; forms layers up to 5 m thick. *Occurrence*: Volume ≪0.001 km^3 (≪0.1%); grades mainly into massive scoria-rich breccia (mScBr).	Clast populations, including spatter rags, are predominantly the juvenile products of an explosive eruption; spatter rags were deformed when hot and small lithics were accidentally incorporated before eruption; spatter-rich layers reflect temporary surging of the current.
mLT Massive lapilli-tuff	*Lithology*: Identical to diffuse-bedded lapilli-tuff (dbLT) (below). *Structure*: Stratification is absent. *Occurrence*: Volume ~0.05 km^3 (~5%). Grades laterally from diffuse-bedded lapilli-tuff (dbLT) and vertically into massive tuff (mT).	Rapid deposition from a granular-fluid-based pyroclastic density current. Massive nature indicates that basal turbulence and traction were suppressed by high basal concentrations.
dbLT Diffuse-bedded lapilli-tuff	*Lithology*: Angular scoria lapilli (≤25%) supported in fine-medium ash matrix; well to moderately sorted; clast populations identical to massive scoria-rich breccia (mScBr). Locally eutaxitic. *Structure*: 5–20 cm-scale, plane-parallel stratification picked out by nodule growth; spatter rags occur in block-rich layer ~1.5 m thick and locally near the base of the lithofacies. *Occurrence*: Volume ~0.25 km^3 (~25%); grades laterally from breccias (mScBr and mTScBr) and vertically into massive tuff (mT).	Rapid deposition from a granular-fluid-based pyroclastic density current; clast populations represent a juvenile eruption population; stratification represents current unsteadiness; block-rich layer containing spatter rags reflects current surge.
bLT and xbLT Thin bedded and cross-bedded lapilli-tuff	*Lithology*: Similar to the diffuse-bedded lapilli-tuff (dbLT) although more variable; poorly sorted; local high concentrations of ignimbrite blocks (≤50 cm) and rare large intraclasts of thinly bedded tuffaceous siltstone (≤3 m long). *Structure*: Stratification commonly undulose and/or laterally discontinuous with some steep (≤45°) cross-stratification and scour-like truncations of stratification; normal and reverse distribution grading defines the stratification. *Occurrence*: Volume ~0.03 km^3 (~3%); conformably overlies massive breccias (mScBr and mTScBr) from which it is gradational.	Deposition from granular-fluid-based density current indicated by poor sorting. Normal and reverse grading record unsteady deposition. Disordered beds, lateral truncations, and scour-and-fill structures reflect extreme current unsteadiness and non-uniformity with repetitive alternations between erosion and deposition; scours represent occurrence of short-lived turbulent vortices at the base of the current. Clast populations generally reflect a juvenile eruption population; ignimbrite blocks are lithics accidentally incorporated into the current.
$mT_{(n)}$ Massive, normal-graded tuff	*Lithology*: Massive, well sorted, medium to fine tuff comprising devitrified glass shards, scoria and pumice fragments. *Structure*: Subtle stratification defined by concentrations of small lapilli (≤4 mm); overall normal grading; dish-and-pillar structures occur locally;	The overall normal grading and otherwise massive nature indicates progressive aggradation from a gradually waning granular-fluid-based current, transitional to deposition from suspension; water escape structures indicate rapid deposition followed by dewatering

Table 1 (continued)

Lithofacies	Description	Interpretation
	contains pods of lapilli-tuff (10–100 cm diameter) indicating extreme soft-sediment disruption. *Occurrence*: Volume ~0.2 km^3 (~20%); grades vertically into white-weathering, very fine-grained massive tuff (vfmT).	during compaction; dewatering may have homogenized the tuff locally; the lapilli-tuff pods indicate extreme soft-sediment disruption.
vfmT Massive very fine-grained tuff	*Lithology*: Massive, white-weathering, very fine-grained, porcellanous tuff; commonly fractured; pods of lapilli-tuff (10–100 cm diameter) occur, particularly towards the top. *Occurrence*: Volume ~0.07 km^3 (~7%); grades vertically from the normal-graded tuff ($mT_{(n)}$); occurs at or near the top of the Pavey Ark deposit, commonly overlain by bed of eutaxitic lapilli-tuff.	Suspension sedimentation of fine ash from a sediment-choked water column; massive nature reflects rapid deposition and/or homogenization due to soft sediment remobilization; pods of lapilli-tuff indicate disruption and incomplete mixing.
empL and empLT Eutaxitic massive pumice lapillistone and lapilli-tuff	*Lithology*: Lapilli-tuff beds, massive ≤30 cm thick; bimodal grain-size distribution with lapilli in a fine tuff matrix; eutaxitic texture defined by flattening of highly vesicular scoria or pumice lapilli. *Occurrence*: Volume ≪0.001 km^3 (≪0.1%); occurs as a 15–30 cm-thick bed at the top of the massive very fine-grained tuff (vfmT), where it forms the top of the Pavey Ark unit, also occurs as pods within the tuff (mT) and porcellanous tuff (vfmT).	Contemporaneous suspension sedimentation of ash and settling of highly vesicular scoria or pumice, which may have floated initially, before sinking when waterlogged. Eutaxitic texture is diagenetic in origin.

below). The subtle gradational layering is readily reconciled with variations in deposition from a slightly unsteady sustained current; it is too subtle, too laterally discontinuous, and too continuously intergradational everywhere across the basin to be due to the arrival of, and deposition from, numerous discrete currents. Throughout the continuous exposures of the breccias and their lateral correlatives, we have found no evidence for a general hiatus in flow or deposition.

The tuff matrix, scoria, pumice and spatter represent juvenile pyroclasts. Small lithic fragments were evidently incorporated within the magma before it was erupted and fragmented to form the spatter. Other lithic clasts (e.g. the rhyolites) may have been incorporated in the conduit or into the current. The morphology of the spatter fragments shows that they were hot and retained considerable ductility during emplacement; some spatter became wrapped tightly around adjacent scoria clasts without any brittle cracking of the outer surface and there are no forms indicating late-stage brittle fragmentation of the spatter. The thin finger-like lobes of spatter that occur between other clasts, and the elongate slab-like fragments, would not have survived intact had the spatter been substantially chilled and hence rigid during emplacement (Fig. 7). The close association of spatter with thick proximal breccias is typical of spatter agglomerates emplaced subaerially at flooded calderas elsewhere (Mellors and Sparks 1991; Branney and Kokelaar 2002 and references therein), although in those cases it is common for the spatter to show evidence of surficial chilling and cracking. We infer that, at least during peaks in mass-flux, lower parts of the current retained a gaseous phase, because the fluidal morphology of the spatter in the coarsest layers (Fig. 7) precludes sustained contact with (liquid) water during emplacement; even brief interaction of hot spatter with liquid water produces surficial cracks due to cooling-contraction and brittle fracturing around a ductile-deforming hot interior (e.g. Mattox and Mangan 1997), yet we have observed no such cracked margins. The retention of heat sufficient for ductile behaviour through to the time of deposition is consistent with a low thermal diffusivity of the juvenile clasts (Thomas and Sparks 1992), but nevertheless requires rapid emplacement directly from an eruption. The coincidence of abundant spatter with the coarsest breccia layers indicates that the arrival of spatter was directly related to peaks (surges) in current competence, but it is unclear whether these peaks related to fluctuating vent conditions or to unsteadiness developed within the current.

The down-current transitions to fines-rich lithofacies (Fig. 10) suggest that much of the ash in the density current overpassed proximal locations. As with other proximal ignimbrite breccias and agglomerates (Druitt 1985; Branney and Kokelaar 2002, p 60), we infer that ash and low-density lapilli were elutriated upwards by interstitial fluid that was displaced vigorously by the rapidly depositing large and dense clasts. Similar subaqueous segregation has been inferred from submarine proximal massive open-work breccias that pass down-current into silt-rich turbidites in Tethyan

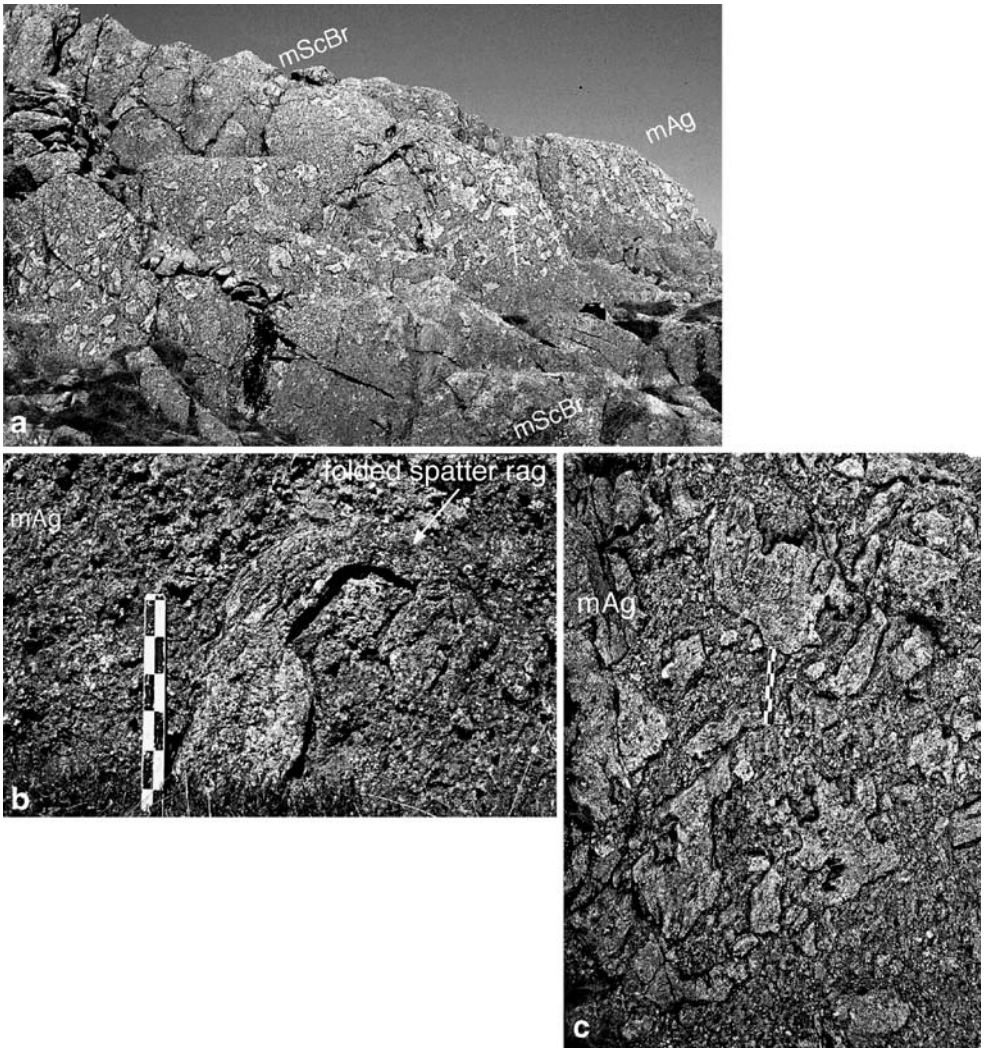

Fig. 7 Massive agglomerate (NY 2839 0790). **a** Spatter concentrated and defining a layer (mAg) within massive scoria-rich breccias (mScBr). Detail shown in **c** is immediately to the left of the metre scale (right centre). **b** Massive agglomerate (mAg) with large spatter fragment folded around a scoria clast. Scale interval is 5 cm. **c** Massive agglomerate showing abundant amoeboid, fluidal-shaped spatter fragments that locally wrap around angular blocks and lapilli; in contrast to spatter at many modern flooded calderas, this spatter is smooth-surfaced and does not show the surficial shrinkage cracks, or deformation-related cracks, or cauliflower-like forms that are typical of chilling interaction with water. Scale ruler is 30 cm

carbonate shelf sediments (Zalasiewicz et al. 1997). The coincidence of the lowest abundance of fine-grained (tuff) matrix with the largest clasts suggests that the most efficient particle segregation by elutriation occurred during surges in competence of the current, when deposition of the largest clasts occurred. The gradational changes in matrix abundance (e.g. transitions between breccia and tuffaceous breccia) probably reflect changing degrees of segregation in response to changing deposition rates and maximum clast size (discussed below). In general, the breccias thin and fine to the west-northwest and rates of deposition and effectiveness of fluid-escape-induced segregation probably declined in this direction (depletive flow of Kneller and Branney 1995).

Massive lapilli-tuff (mLT)

Description Massive lapilli-tuff comprises moderately to poorly sorted, fine to coarse tuff supporting angular lapilli of variably vesicular andesite. There is no discernible stratification (Fig. 9a). The clast types are the same as those in the massive breccias (mScBr and mTScBr), although spatter is rare. Massive lapilli-tuff commonly grades both laterally and vertically into diffuse-bedded lapilli-tuff (dbLT).

Interpretation This ignimbrite lithofacies was deposited from a sustained granular-fluid-based density current that contained abundant ash. As with massive ignimbrite (Branney and Kokelaar 2002) and massive turbidite divisions elsewhere (Kneller and Branney 1995), the absence of sedimentary structures suggests that deposition was from a fluid-escape-dominated flow-boundary zone, in which high clast concentrations suppressed turbulence and tractional processes, and in which both the lowermost part of the current and the uppermost part of the deposit were poorly packed, 'quick' (low strength) dispersions. There is no direct evidence regarding the presence or absence of gas in the interstitial fluid at the depositional flow boundary.

Diffuse-bedded lapilli-tuff (dbLT)

Description Diffuse-bedded lapilli-tuff is very similar to the massive lapilli-tuff (mLT; described above) into which it grades, except that it exhibits impersistent, very diffuse, 5–20 cm-thick planar beds (Fig. 8a, b). The diffuse beds are generally too subtle to distinguish except where emphasized by concentrations of authigenic epidote (Fig. 8b), the hydrothermal-diagenetic growth of which was evidently influenced by subtle variations in grain-size or permeability related to matrix sorting. In the vicinity of the Scafell Dacite lava dome, rounded pebbles of dacite occur in discontinuous thin layers on internal surfaces marking local non-deposition or erosion (e.g. at 22 m on log 6; at 18 m on log 1, Fig. 10a).

Lithofacies dbLT commonly grades upwards, over a few metres, from underlying massive breccias (mScBr and mTScBr) and also into overlying massive tuff with

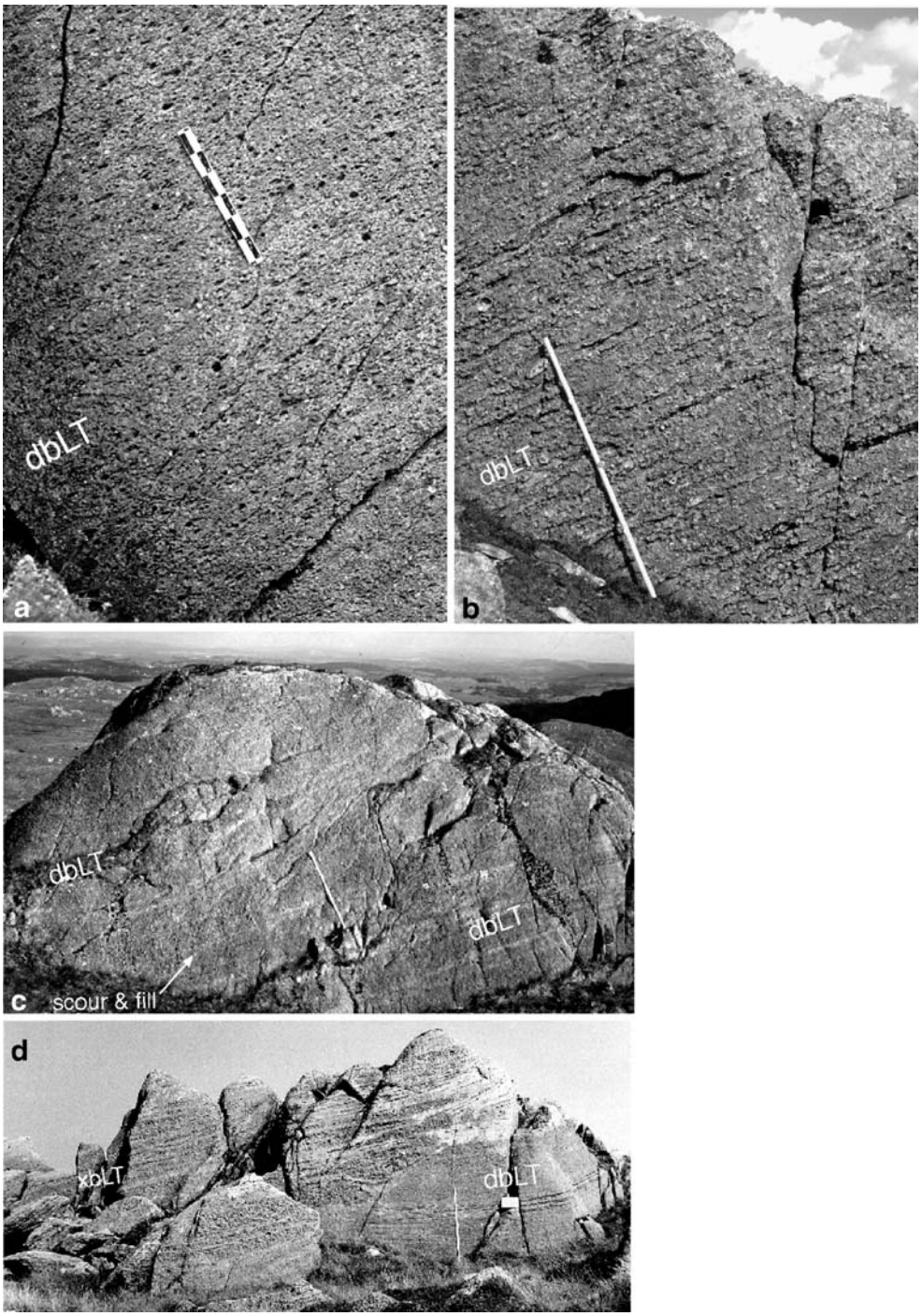

Fig. 8 Diffuse-bedded, thin-bedded and cross-bedded lapilli-tuff in the Pavey Arc ignimbrite. **a** Eutaxitic massive to diffuse-bedded lapilli-tuff (dbLT). The fiamme, predominantly recess-weathered, are diagenetically flattened pumice lapilli; scale ruler is 30 cm (NY 2223 0677). **b** Diffuse-bedded lapilli-tuff (dbLT); diffuse bedding is emphasized by epidote (NY 2474 0640; at 18 m on log 8). **c** Diffuse-bedded lapilli-tuff on left-hand side infilling scour 1.5 m deep (NY 2840 0802). *Arrow* marks cross-cutting scour surface. **d** Diffuse-bedded and cross-bedded lapilli-tuffs (dbLT, xbLT); internal scour cuts >1 m into diffuse-bedded lapilli-tuff (dbLT) and is filled with variously cross-bedded lapilli-tuffs. Scour surfaces nearby are steeper (≤45°); scale ruler is 1 metre (NY 2840 0802)

normal-grading ($mT_{(n)}$). It is commonly intergradational laterally and vertically with massive lapilli-tuff (mLT) and in places it includes metre-scale layers of eutaxitic massive lapilli-tuff and eutaxitic diffuse-bedded lapilli-tuff (emLT and edbLT; Fig. 8a).

Interpretation The broad similarity and intergradational nature of this ignimbrite lithofacies with massive lapilli-tuff (mLT) suggests a broadly similar mode of deposition. The poor sorting and subtle diffuse nature of the bedding are not typical of tractional stratification; deposition is inferred to have been similar to that for mLT, except with slight unsteadiness, possibly originating spontaneously within the sustained current. The characteristics may have arisen where clasts in lowermost parts of the current had a somewhat greater tendency to become frictionally locked in layers. As inferred for dbLT elsewhere in subaerial ignimbrites (e.g. Brown and Branney 2004), frictional locking would happen when there was less vigorous fluid-escape and enhanced grain–grain interactions. Such conditions require slightly lower rates of particle supply to the flow-boundary zone or slightly higher rates of flow-boundary shear than for massive lapilli-tuff (Branney and Kokelaar 2002, p. 43), although not sufficient for full development of grainflow-dominated deposition, which tends to produce better-developed segregation of different sized clasts and more distinct bedding (e.g. Sohn 1997). The appropriate conditions must have been sustained for a considerable time to aggrade the great thicknesses attained by this lithofacies. The diffuse metre-scale layers of eutaxitic lapilli-tuff (edbLT) suggest more marked depositional unsteadiness, with entrapment of abundant pumice and highly vesicular scoria clasts that were later flattened during burial and diagenesis.

The rounded pebbles of dacite near and at the top of this lithofacies contrast markedly with the angular shapes of most other clasts, and they are not likely to have been rounded during emplacement. Their location and association with scours indicate that they were probably incorporated into the current from a former or extant shoreline deposit of pebbles on the nearby Scafell Dacite lava dome (explained below).

Thin-bedded and cross-bedded lapilli-tuff (bLT; xbLT)

Description The thin-bedded and cross-bedded lapilli-tuff lithofacies are generally poorly sorted (Fig. 8c, d), although the proportion of fine tuff matrix varies widely and the lithofacies locally grade into thin-bedded lapillistone. Clast types are similar to those in the massive breccias (mScBr and mTScBr), but spatter fragments are absent. Concentrations of lithic clasts occur locally, with angular to rounded blocks of welded ignimbrite (≤50 cm) and slabs of tuffaceous siltstone, up to 3 m long.

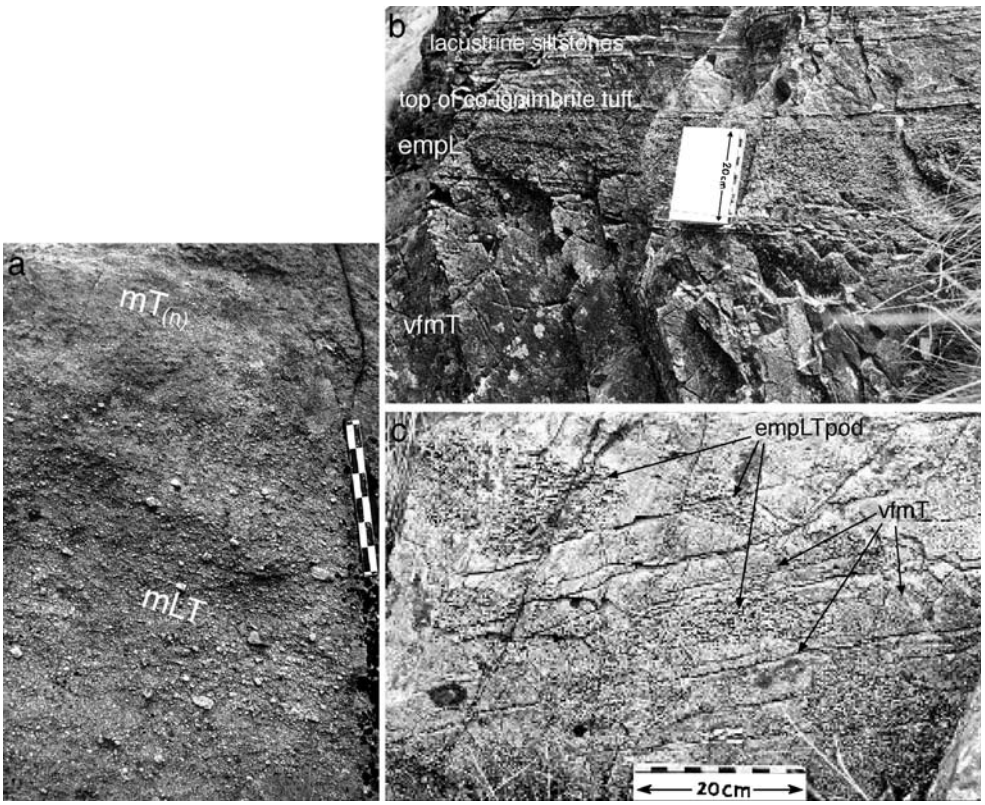

Fig. 9 Lithofacies of upper, normal-graded parts of the Pavey Arc unit. **a** Massive lapilli-tuff (mLT) grades up into massive tuff with normal grading ($mT_{(n)}$); scale ruler is 30 cm (NY 2610 1120). **b** Bed of eutaxitic massive pumice lapillistone (empL) overlies massive, very fine tuff (vfmT) at the top of the Pavey Arc unit. Overlying beds are lacustrine sandstone and siltstone (NY 2358 0957). **c** Pods of eutaxitic massive pumiceous lapilli-tuff (empLT-pod) within very fine massive tuff (vfmT), indicative of soft-state disruption (NY 2397 0647)

Thin bedding is laterally discontinuous, commonly undulose, and is defined by normal and reverse distribution grading and variations in sorting. Dune-type cross-stratification is not apparent, and determination of the current direction is not possible. Instead, the lithofacies appear disordered and dominantly form successive scour-and-fill packages (Fig. 8c, d). Discordant scour surfaces, as steep as ≤45°, are common and some scour-and-fill structures ≤2 m deep are filled with 9–30 cm-thick sets of steep (30–45°) cross-strata (e.g. at 25 and 35 m on log 15 and 117 m on log 14 in Fig. 10a).

Interpretation The complex grading patterns, undulose thin impersistent bedding, and scour-and-fill structures of lithofacies bLT and xbLT indicate rapid, unsteady and non-uniform fluctuations between deposition and deposit remobilization. The geometry, poor sorting, and diverse grading in the cross-strata are inconsistent with dune migration due to tractional deposition from the bed-load of a fully dilute current. Rather, the poor sorting and absence of tractional stratification suggest that turbulence-induced traction and winnowing were largely suppressed by high clast concentrations in the lowermost parts of a granular-fluid-based density current. The bedding and distribution grading suggest that granular flow and segregation processes were important (granular-flow-dominated flow-boundary zone of Branney and Kokelaar 2002). During overall aggradation, localised increases of shear stress applied by the current caused repeated re-entrainment of particles that had just been deposited; such localised current surges may have been transient impacts of metre-scale vortices capable of sweeping momentarily through the lowermost, granular-fluid part of the current. Closely similar scour-and-fill structures occur in marine volcanogenic turbidites at Snowdon caldera, where they are interpreted to have been formed by currents that debouched from narrow submarine canyons and mainly overpassed a depositional fan-head (Kokelaar 1992). They have also been reported in lahar deposits and in subaerial ignimbrites (Branney and Kokelaar 2002, p. 110–113; Brown and Branney 2004). As in these examples, the local steep attitude of scour surfaces reflects transient support by the high-concentration lowermost parts of the current prior to almost immediate burial in the wake of the passing local vortex or surge. In the Pavey Arc case, there is no evidence bearing on the gaseous or aqueous nature of the interstitial fluid in the depositional flow-boundary zone of the current.

The rare blocks of welded ignimbrite are similar to the caldera-fill ignimbrites that underlie the caldera-lake succession. They may have been incorporated in the eruption conduit or by the density current from a nearby fault scarp or canyon wall. Similarly, the siltstone intraclasts were probably derived from partially lithified caldera lake sediments exposed somewhere up-current.

Normal-graded massive tuff ($mT_{(n)}$)

Description This lithofacies comprises coarse to fine tuff, with normal grading across its entire thickness (up to several tens of metres). It is gradational into underlying lapilli-tuffs (mLT (Fig. 9a) and dbLT) and overlying very fine massive tuff (vfmT). Stratification is absent at most locations, although very subtle layering is discernible locally where the tuff contains sparse fine lapilli and where emphasised by epidote alteration; some indistinct laminae occur in fine-grained upper parts. Dish-and-pillar structure is common and the lithofacies locally hosts some pods, 10–100 cm in diameter, of eutaxitic lapilli-tuff (e.g. at 14 m on log 4 and at 38 m on log 1 in Fig. 10a). The tuff mainly comprises shards and variably vesicular fine scoria and pumice fragments, but original vitroclastic textures have been widely obliterated by recrystallization.

Interpretation The normal grading from poorly sorted lapilli-tuff (mLT and dbLT) beneath suggests deposition from a waning current. The predominantly massive character suggests that tractional deposition was inhibited by some combination of (1) high ash concentration in lowermost parts of the current, (2) low shear stress on the bed, and (3) high rates of deposition from suspension (Arnott and Hand 1989; Vrolijk and Southard 1998), ultimately leading to development of a direct-fallout-dominated flow-boundary zone (Branney and Kokelaar 2002). Dish-and-pillar structure indicates that the original ash was loosely packed, such that rapid deposition or seismic shock caused expulsion of pore water. The pods of eutaxitic lapilli-tuff indicate liquefaction-related foundering of an overlying pumice-rich layer, or intercalated lenses, possibly also triggered by seismic shock or via instability due to movement on volcanotectonic faults (see below). The absence of any relics of distinct stratification indicates that the lithofacies was predominantly massive prior to dewatering and disruption.

Very fine-grained massive tuff (vfmT)

Description This lithofacies comprises massive, white-weathering, very fine to extremely fine tuff, with a surface appearance and feel reminiscent of porcelain (Fig. 9b, c). Original microscopic textures are mostly obliterated by recrystallization, but devitrified shards and small scoria and pumice fragments are preserved in places. Some indistinct, discontinuous planar laminae occur towards the top and

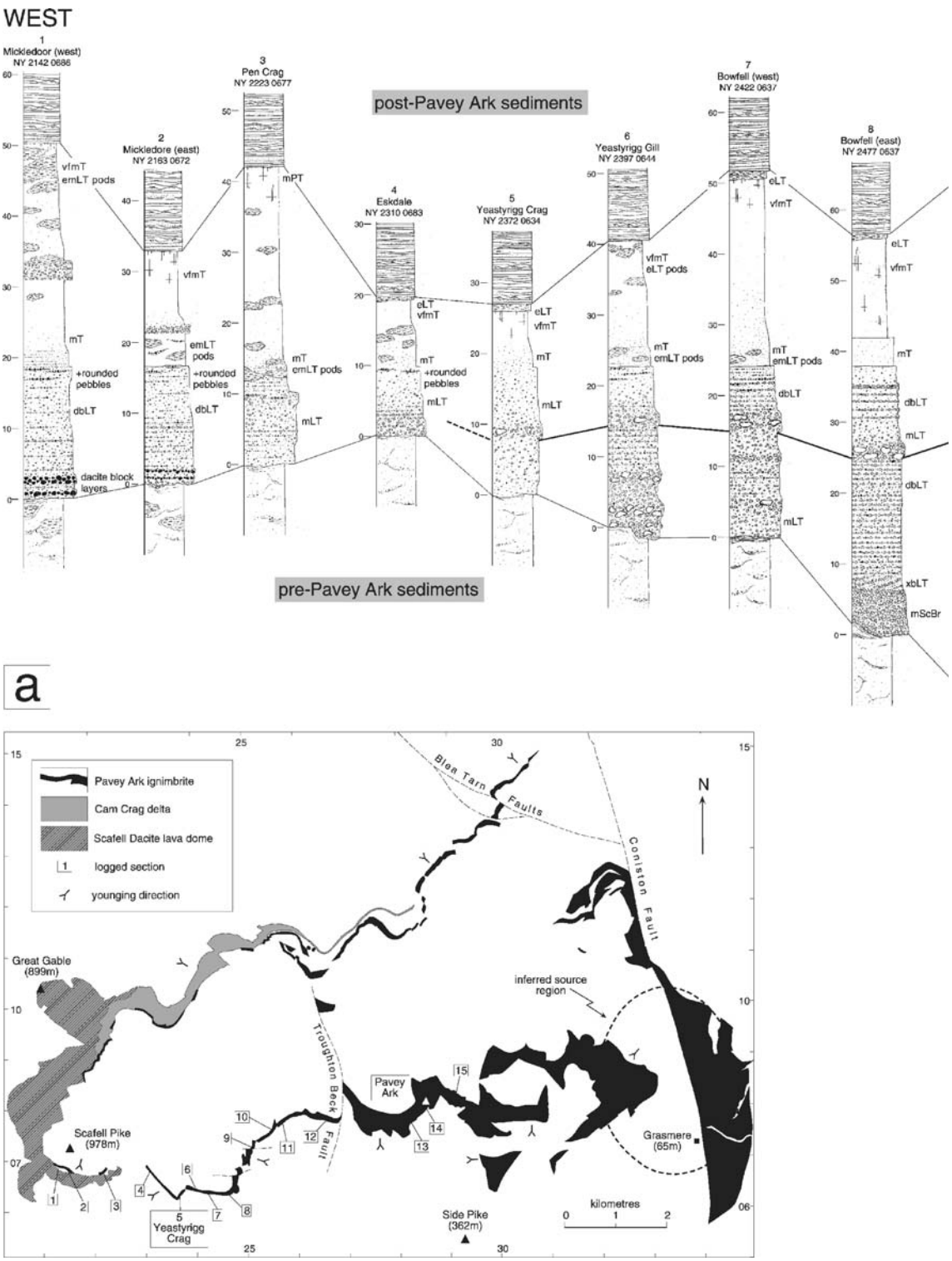

Fig. 10 Logs representative of the Pavey Ark ignimbrite and co-ignimbrite tuff at 25 localities around the Scafell caldera. **a** Southern part of caldera. **b** Northern part of caldera. Inset simplified map shows the Pavey Ark unit and location of the logged sections. In the south-west, the ignimbrite rests against the Scafell Dacite lava dome; in the north-west it rests on the Cam Crag fan-delta, which prograded into the caldera lake from the north-west (see text). Map coordinates are from the UK Ordnance Survey National Grid Square NY

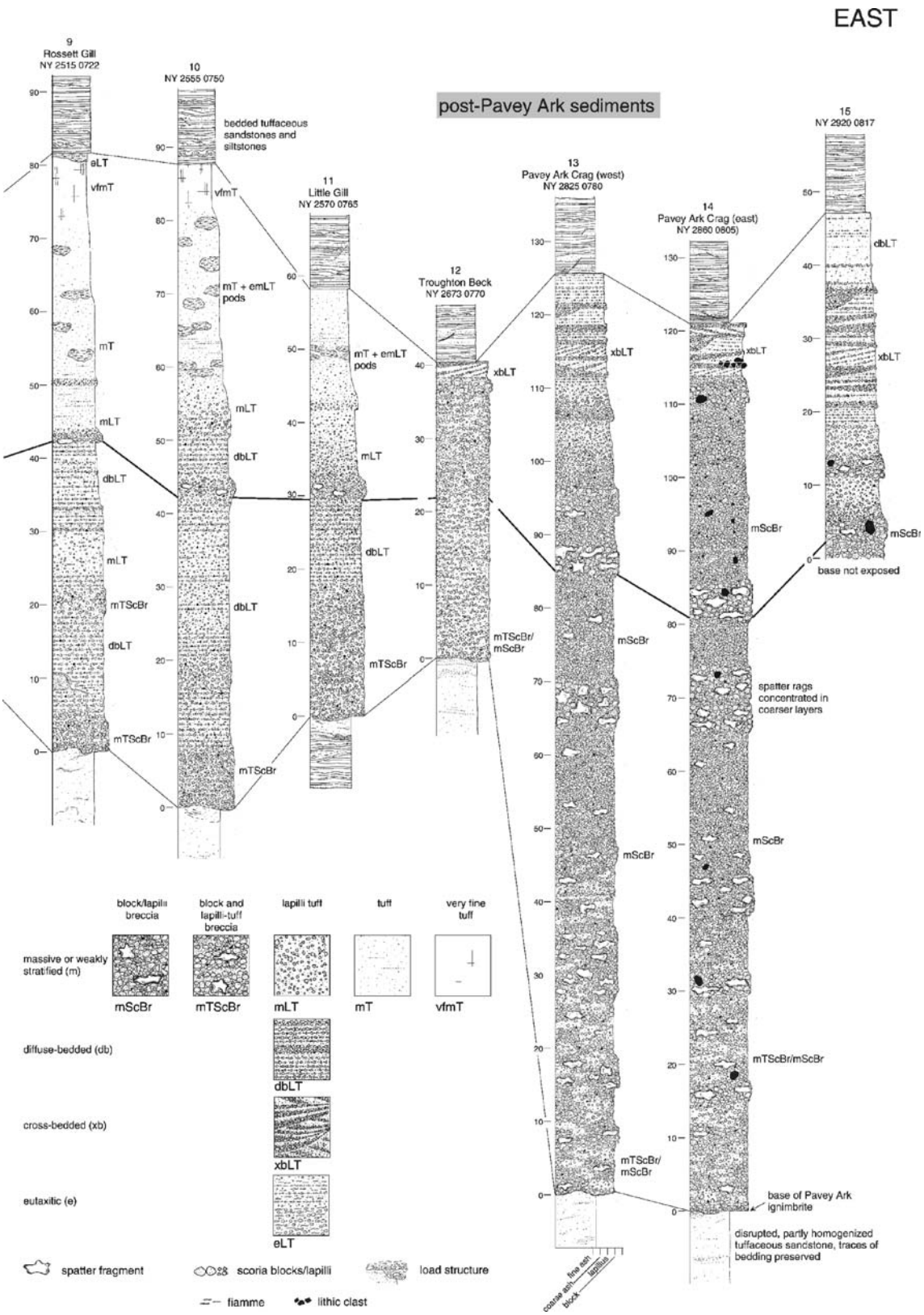

Fig. 10 (continued)

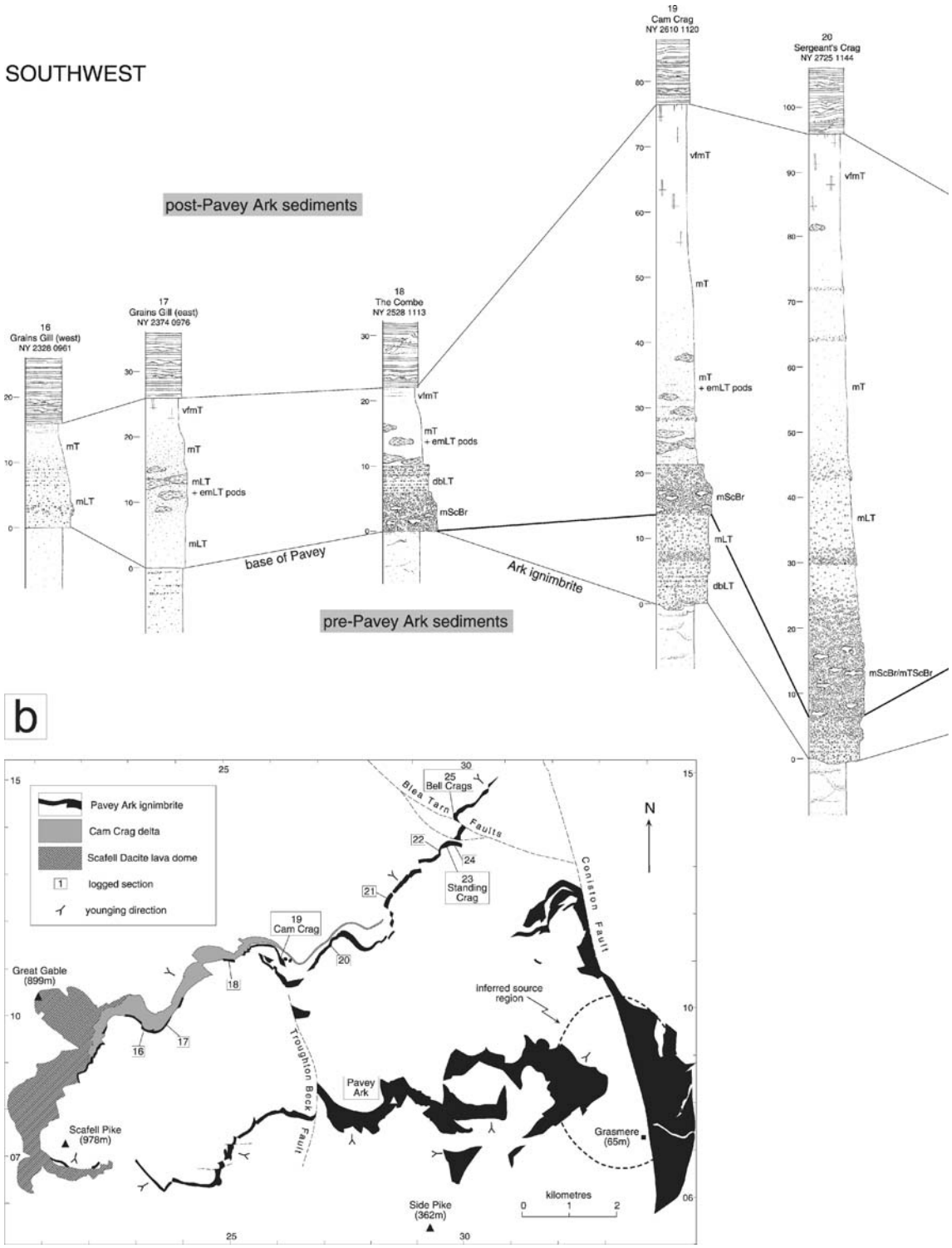

Fig. 10 (continued)

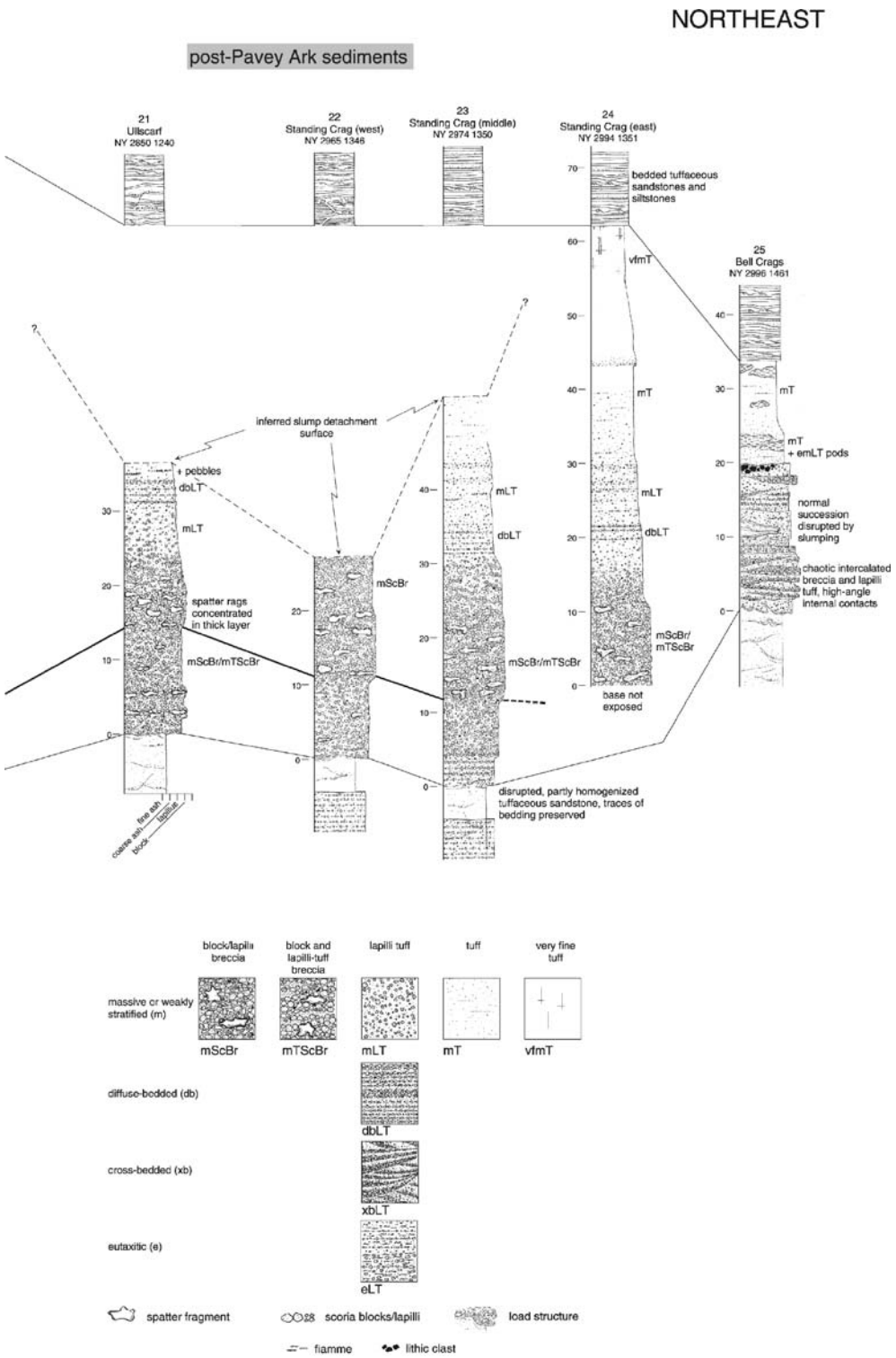

Fig. 10 (continued)

pods of eutaxitic lapilli-tuff (10–100 cm diameter; Fig. 9c) are common (e.g. at 40 m on log 6 in Fig. 10a).

Very fine-grained massive tuff grades from massive graded tuff ($mT_{(n)}$) beneath, and commonly forms the top of the Pavey Ark deposit. Its upper contact is sharply defined, either by a bed of eutaxitic lapillistone or eutaxitic lapilli-tuff (empL or empLT; Fig. 9b), or by the base of the overlying (background) lacustrine sedimentary succession (Figs. 4 and 9b).

Interpretation Very fine-grained massive tuff represents settling of ash suspended in water unaffected by any pronounced lateral current. The large thicknesses of this massive lithofacies, up to 30 m, and its gradation from underlying massive normal-graded tuff ($mT_{(n)}$), suggest that it is unlikely to have accumulated by Stokes' Law (slow) settling from a dilute suspension; it is more likely to represent relatively rapid aggradation from a sediment-choked water column. Weak currents, possibly widely convective and due to temperature or suspension-load variations in the lake, might have influenced the settling. Some of the indistinct laminae may be due to lateral deflections of descending plumes that formed from particle-concentration inhomogeneities in the choked column (e.g. Carey et al. 1988; Carey 1997; Manville and Wilson 2004). Initial loading-related compaction of the thick deposit would have been slow and expulsion of pore water would have hindered late settling (Druitt 1995). There is evidence that the ash locally became thickly ponded within (caldera-collapse-related) depocentres that formed during sedimentation (explanation below), which indicates some lateral flow. The eutaxitic lapilli-tuff pods indicate soft-sediment mobilization of formerly pumice-rich layers, and it is possible that some localised primary lamination has been obliterated.

Eutaxitic lithofacies (empL; empLT)

Description Within both the normal-graded and the very fine-grained massive tuffs ($mT_{(n)}$ and vfmT) there are lenses, pods and layers in which slightly flattened to strongly flattened lapilli (fiamme) are set in a very fine tuff matrix (Fig. 9c), giving a marked bimodal grain-size distribution. Equant dense andesitic lapilli are characteristically absent from these lithofacies, and flattened shards are not seen within the fine matrix. A single bed of empL or empLT, 15–30 cm thick, occurs widely at the very top of Pavey Arc unit (Fig. 9b).

Interpretation The strongly bimodal sorting indicates contemporaneous deposition of two distinct clast populations with contrasting hydrodynamic behaviours. The flattened clasts were lapilli of highly vesicular scoria and pumice that were neutrally buoyant or floated initially, before sinking when waterlogged. Their flattened shapes record burial-compaction following diagenetic alteration to clays (e.g. Branney and Sparks 1990); there is no evidence for welding. The inference of late sinking implies that the vesicular lapilli were cold on contact with water, so that they absorbed water relatively slowly; hot pumice clasts sink rapidly on encountering water, because the quench-cooling causes the contained hot gas to contract or condense so that water is sucked into the microvesicles (Whitham and Sparks 1986). The eutaxitic pods (mpL and empLT) within the massive tuffs are remnants of pumice-rich layers or lenses that became disrupted during liquefaction.

Interpretation of lithofacies architecture

Excellent exposure allows the spatial variations within the Pavey Arc unit to be resolved in considerable detail. We present the variations on 25 logs (Fig. 10) and in two schematic transects roughly 4 km apart (Fig. 11). The contact between the lapilli-tuffs (dbLT and mLT) and the massive, normal-graded tuff ($mT_{(n)}$) is set to horizontal on Fig. 11. This restores to nearly horizontal a distinctive spatter-rich layer that occurs towards the top of the breccia and is traceable for ~6 km westwards into lapilli-tuff (e.g. from 82 m on log 14 to 9 m on log 5 in Fig. 10a). In the south-east, where normal-graded tuff ($mT_{(n)}$) is absent, the horizontal is taken at the base of the cross-bedded lapilli-tuff (xbLT).

Source vent area

In the main study area, the Pavey Arc ignimbrite is thickest and coarsest, with most abundant spatter, in the south-east, around Pavey Ark (Figs. 6a and 7). Its source is inferred to be 5 km east of Pavey Ark, in the vicinity of the Coniston Fault near Grasmere (Figs. 2 and 10), where ≥500 m of mainly coarse, massive breccias (mScBr and mTScBr) and agglomerate (mAg), with some lapilli-tuff (mLT) and eutaxitic lithofacies (empLT), are cut by abundant irregular-shaped andesite intrusions.

Fining upwards

At most locations the lacustrine Pavey Arc unit shows overall normal grading. Massive breccias (mScBr, mTScBr) typically grade upwards through lapilli-tuffs (mLT and dbLT) and coarse, medium, fine and very fine tuffs ($mT_{(n)}$, vfmT) (Figs. 10 and 11). Sharp contacts between lithofacies are uncommon (e.g. 38 m on log 8 and 23 m on log 6). The overall normal grading is less well developed nearer to the eruptive source in the south-east

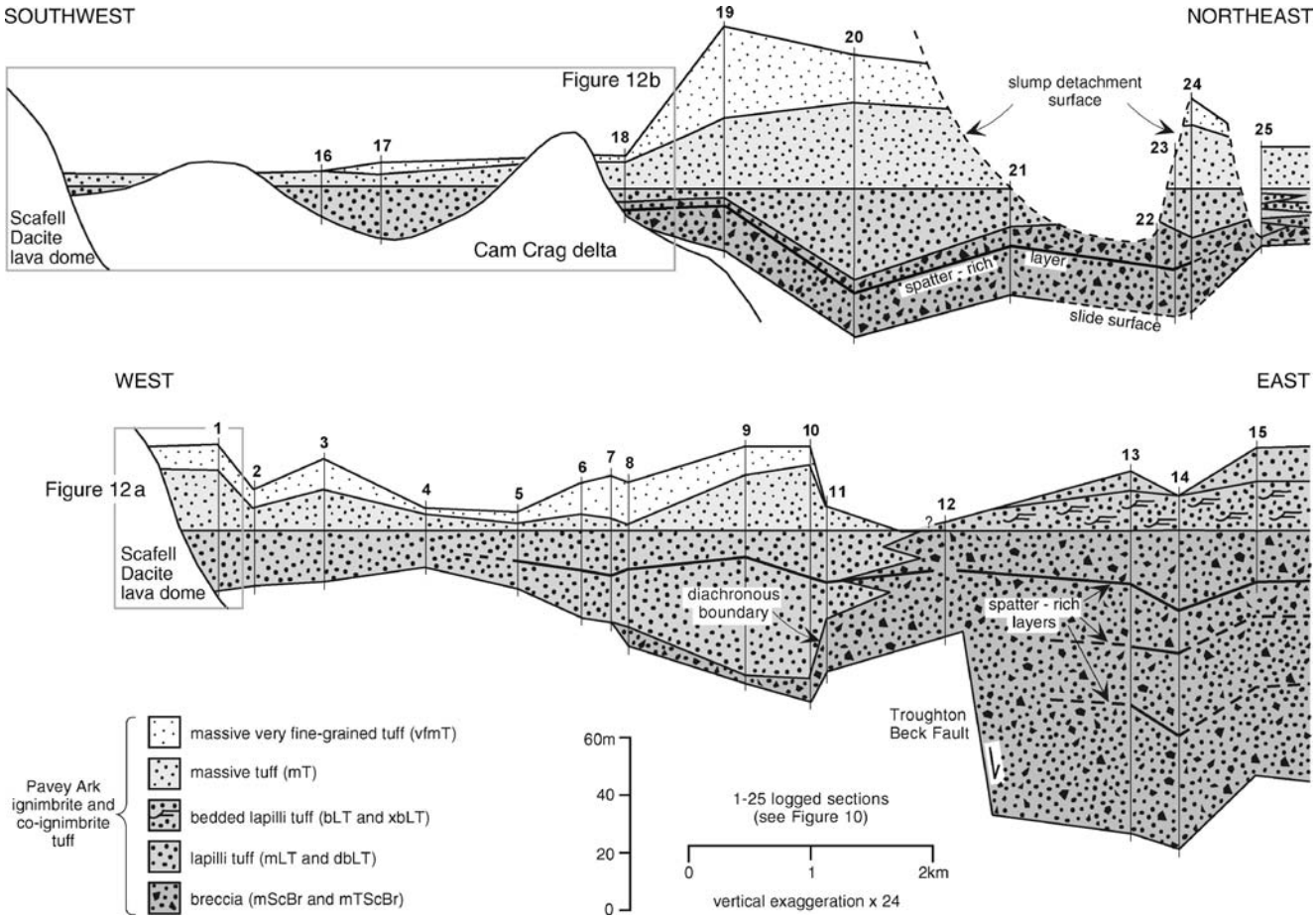

Fig. 11 Lithofacies architecture of the Pavey Ark ignimbrite and co-ignimbrite tuff, based upon the 25 logs shown in Fig. 10; the locations of Fig. 12a, b are indicated. Note the vertical scale exaggeration (x24)

(where the fine tuff is absent; logs 12–15, Fig. 10a), and it is best developed distally, in the north and west. The normal grading is taken to indicate that the ignimbrite was deposited from a sustained current that gradually waned in competence until it ceased, when ash remaining in the water column settled out of suspension to form the co-ignimbrite ash deposit at the top. We cannot clearly distinguish a boundary between the top of the ignimbrite and its associated co-ignimbrite ash deposit. We can assign the lapilli-tuff (mLT) and coarse-grained lower parts of the massive tuff (mT) to deposition during waning phases of the main current, but the generally smooth gradation up into very fine-grained tuff (vfmT) gives no hint of when sedimentation became dominated by fallout from the overlying water column, rather than from the very last part of the current. The sedimentation through this transition must have involved significant hindered settling and occurrence of a thick and potentially mobile 'quick' bed, which is radically different from the sedimentation of co-ignimbrite ash associated with subaerial pyroclastic currents. We take all of the fine- and very fine-grained massive tuff (mT, vfmT) to represent co-ignimbrite ash; it constitutes some 25% of the studied Pavey Arc unit.

Longitudinal variations

The lacustrine Pavey Arc ignimbrite thins and becomes finer grained distally, towards the west-northwest. The coarsest and thickest breccia, in the south-east, contains the highest concentrations of spatter and large lithic blocks (e.g. silicic welded ignimbrite blocks). The coarse, fines-poor breccia and agglomerate (mScBr, mAg) thin dramatically from >100 to <10 m across the Troughton Beck Fault, grading laterally, westwards, through somewhat finer and less well sorted breccia with only sparse spatter (mTScBr) into lapilli-tuff (dbLT and mLT) (Figs. 10 and 11). One spatter-rich layer in particular can be traced widely through this lithofacies variation. Although inevitably there would have been a time interval between the arrival of abundant spatter at proximal locations and its arrival at distal locations to form a single layer, this interval was probably brief compared with the total duration of deposition. Hence,

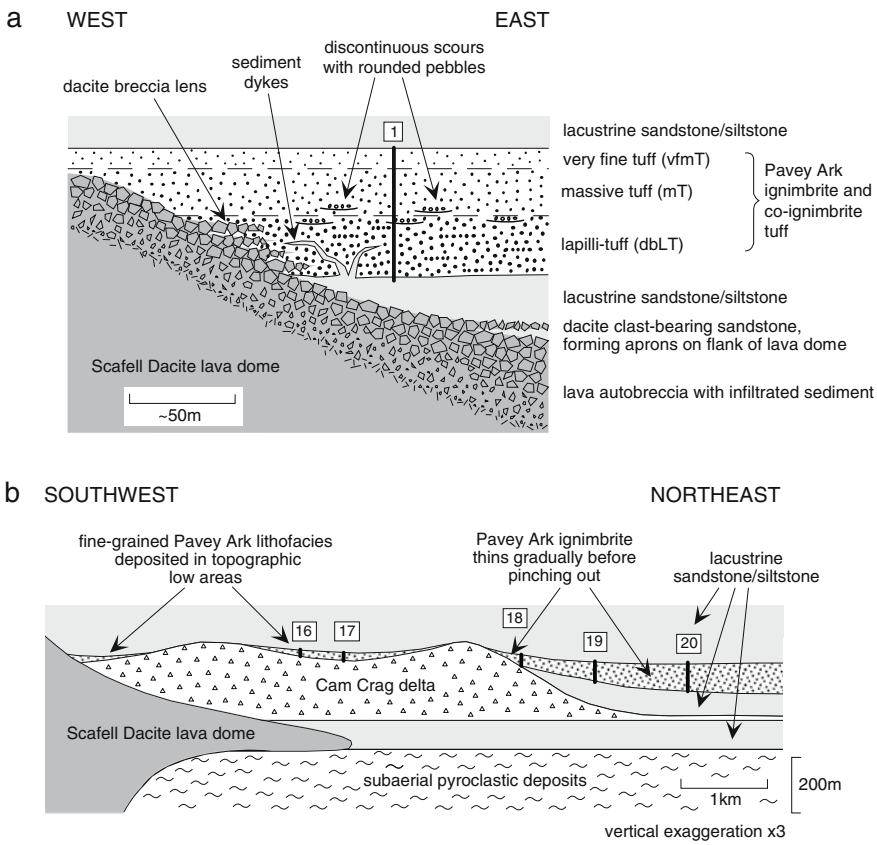

Fig. 12 Onlap relationships of the Pavey Ark ignimbrite and co-ignimbrite tuff. **a** Against the Scafell Dacite at Mickledore, near Scafell Pike (NY 2130 0685). **b** Onto progradational pebbly breccia and coarse sandstone of the Cam Crag fan-delta (NY 25 11)

each spatter-rich layer constitutes a near-instantaneous time-surface (*entrachron* of Branney and Kokelaar 2002). The uppermost spatter-rich layer (Figs. 10 and 11) defines an entrachron that cuts across the lithofacies boundary between the breccia and the lapilli-tuff. It proves a temporal (longitudinal) correlation between the proximal breccias and the more distal lapilli-tuffs and it shows that the lithofacies boundary is strongly diachronous and shifts sourcewards with stratigraphic height (Fig. 11). Similar diachronous architecture is recorded in subaerially emplaced proximal ignimbrite breccia (e.g. Walker 1985; Druitt and Bacon 1986).

The pyroclastic density current that deposited the ignimbrite was depletive (*sensu* Kneller and Branney 1995); its competence, as registered by the maximum size of dense clasts it could transport, decreased with distance from source as the current spread out across the lake floor (divergent flow). Through time, as the current waned, the distance to which the current could transport blocks progressively diminished, so that the farthest limit of breccia deposition migrated sourcewards (Fig. 11).

The uppermost part of the Pavey Ark unit is mostly very fine massive tuff (vfmT) with no obvious longitudinal variations. However, proximally, around Pavey Arc (Fig. 10), the uppermost deposits are diffuse-bedded, thin-bedded and cross-bedded lapilli-tuff (dbLT, bLT, xbLT). These deposits are up to 35 m thick, but thin distally and pinch out within 6–8 km of the inferred source.

Interaction with lake-floor topography

In western and north-western parts of the caldera lake, the Pavey Arc density current interacted with lake-floor topography created by a steep-sided lava dome and an inactive gravel delta (Figs. 10 and 11).

The Scafell Dacite lava dome, extruded before development of the lake, has a flow-banded interior that grades outwards into coarse autoclastic breccia with a fine-grained, infiltrated, lacustrine sedimentary matrix (Figs. 5c and 12a). The ignimbrite in this vicinity comprises some 20 m of diffuse-bedded lapilli-tuff (dbLT) that grades up into 25 m of massive, normal-graded and very fine massive tuff ($mT_{(n)}$ and vfmT). Several beds of angular dacite clasts derived from the lava dome thin and wedge-out away from it within the diffuse-bedded lapilli-tuff (Fig. 12a). Farther from the dome (within 1 km), discontinuous scour surfaces with lags of rounded dacite pebbles occur within and just above the diffuse-bedded lapilli-tuff (e.g. at 18 m on log 1, 16 m on log 2 and 9 m on log 4 in Fig. 10a). The scours and associated rounded pebbles do not occur elsewhere.

The angular dacite clasts within the lapilli-tuff record repeated incorporation of autoclastic debris from the lava-

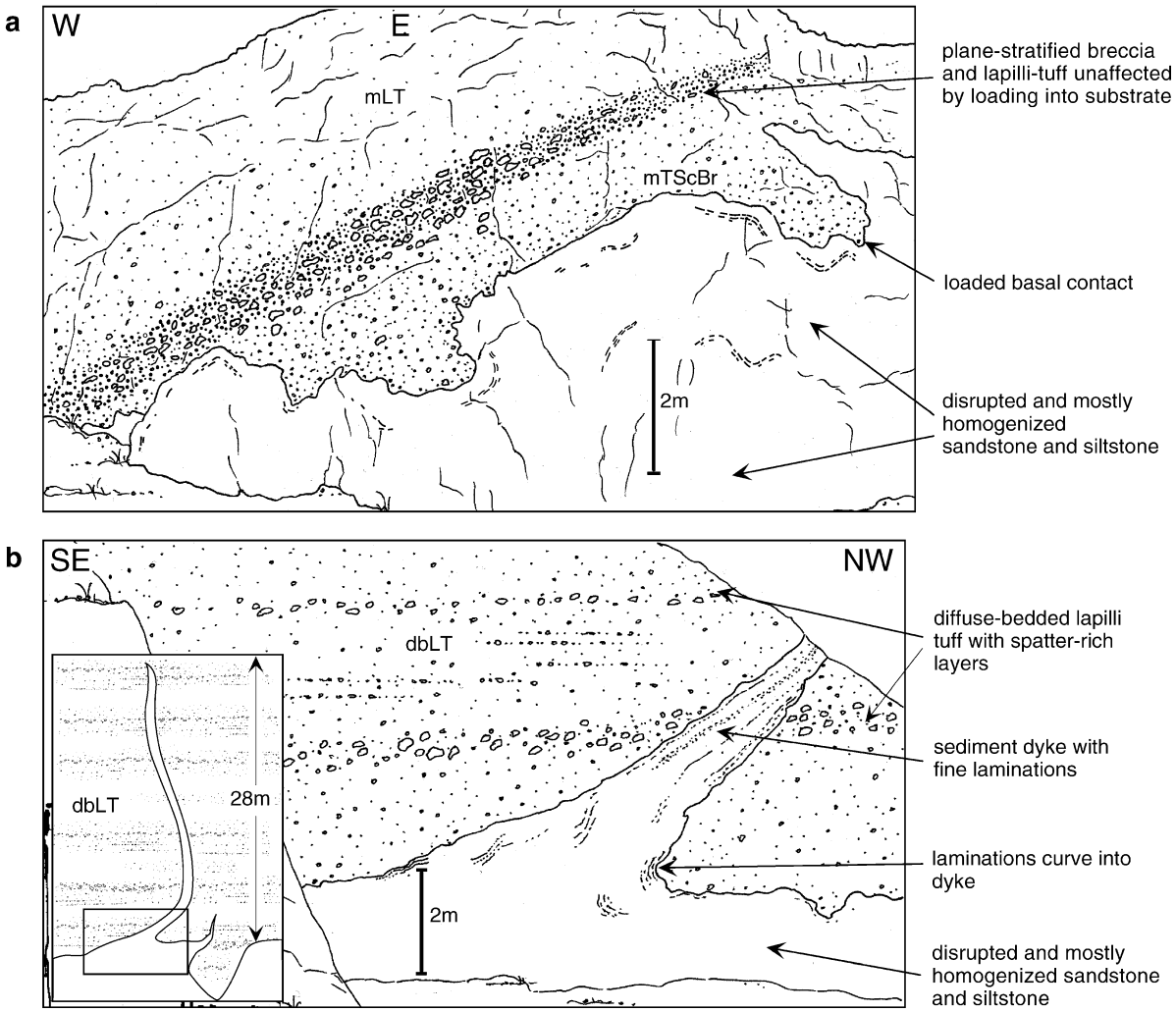

Fig. 13 Consequences of syn-sedimentary loading-related deformation of the substrate of the Pavey Ark ignimbrite. **a** Basal contact at Yeastyrigg Gill, showing deformation that occurred early during ignimbrite deposition (NY 2397 0644). **b** Basal contact with sediment dyke at Cam Crag, showing deformation that occurred at an advanced stage of ignimbrite deposition; *inset* shows full extent of sediment dyke (see text; NY 2618 1115)

dome flank into the current, during progressive aggradation of the ignimbrite. The rounded pebbles of dacite were probably derived from pebbly lake-shore deposits also occurring on the flank of the dome. The association of the pebbles with discontinuous scours in the vicinity of the dome suggests that the density current entrained pebbles when parts of it, or related seiche waves, ran up and were reflected or drained back across contemporary or earlier shoreline deposits; the pebble-bearing current interfered with the sustained on-coming current, causing localised turbulence with scouring and bed-load deposition of pebble lags.

Prior to the Pavey Arc eruption, a 275 m-thick fan-delta or Gilbert-type delta (Cam Crag delta in Figs. 10, 11 and 12) had prograded into the lake from the north-west, partially burying the Scafell Dacite lava dome. It comprised pebbly breccia and coarse sand, and it formed a slope dipping at 8–15° to the south-east (Kneller and McConnell 1993). Other lake deposits buried lower parts of this slope, but successive lithofacies of the ignimbrite and co-ignimbrite deposit show onlap on to upper parts of it (Figs. 11 and 12b). Breccias (mScBr and mTScBr) bury it across a distance of over 1.5 km, progressively thinning and becoming finer-grained upslope before pinching out, and the upper, finer grained lithofacies (mLT, $mT_{(n)}$ and vfmT) of the ignimbrite and co-ignimbrite deposit overlap these coarse lithofacies, extending farther up the delta slope and infilling depressions between delta lobes.

The partially draped slope of the old delta deflected the pyroclastic density current, causing it to decelerate and deposit a proportion of the larger blocks that were being carried predominantly within its lowermost levels. The current was increasingly depleted in blocks with distance up the slope and those parts that surmounted the entire slope carried only lapilli and ash. The lake floor topography effectively caused flow-stripping of the higher, more dilute

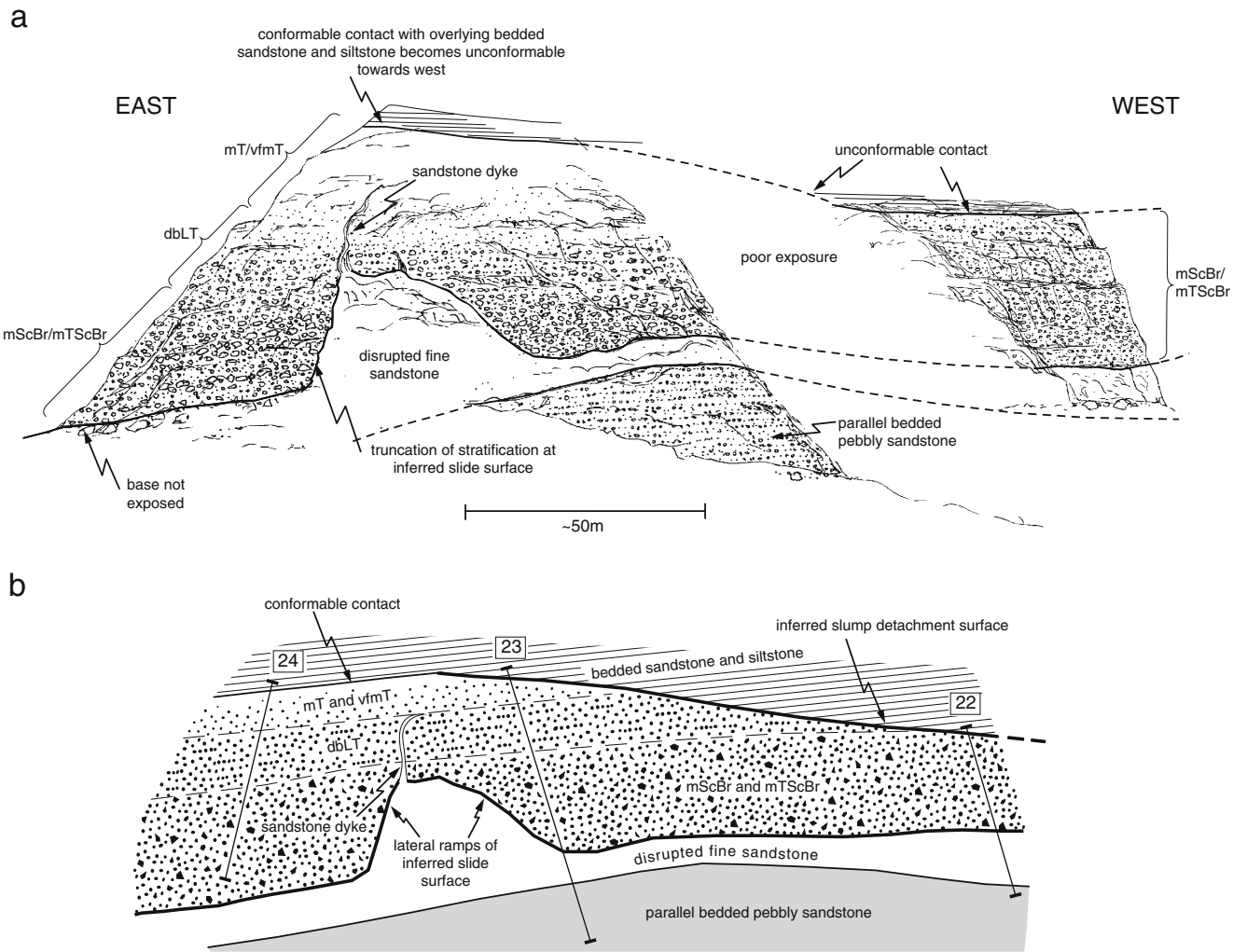

Fig. 14 Field relationships due to sliding and slumping of the Pavey Ark ignimbrite and co-ignimbrite tuff, at Standing Crag (see text; NY 298 135). **a** Field sketch. **b** Diagrammatic explanation of field sketch

and finer-grained parts of the current, which continued to surmount the slope to heights of at least 60 m. Topographic restriction accompanied by flow-stripping of upper parts of density stratified currents has been inferred from marine turbidites (e.g. Piper and Normark 1983) and from subaerial pyroclastic deposits (Fisher 1990; Fisher et al. 1993; Loughlin et al. 2002). In the case of the Pavey Arc density current, the stripping process must have been sustained, because it spanned the period during which the massive breccia progressively aggraded. It is not clear how much of the height attained was the result of momentum-driven run-up as opposed to merely representing the thickness of the density stratified current (e.g. Muck and Underwood 1990). Experiments have shown that a steep slope oriented normal to the direction of a high-concentration, coarse-grained density current causes blocking with substantial localised deposition, whereas a gentle slope and a more oblique angle of incidence favour deflection with a less marked sedimentary response (Alexander and Morris 1994; Woods et al. 1998). We find no substantial thickening of the Pavey Ark ignimbrite at the lava dome or the gravel delta, and we infer that lower parts of the current were mainly deflected at both, rather than substantially blocked.

In general, the primary outbound Pavey Ark current must have been influenced by blocked or reflected currents to some extent, because the outbound current duration is likely to have been of the order of an hour to several hours (see below), whereas, at ~10 m s^{-1}, the front of the outbound current would have crossed the basin floor to the Scafell Dacite lava dome in less than 15 min and to the putative western margin of the caldera in some 30 min. However, except for the case where pebbles are associated with localised scouring within 1 km of the lava dome, as described above, there is no clear signature of reflected currents in the mainly massive deposit. Counterflows may have been less-concentrated and hence over-ridden the oncoming flow, or internal waves may have

been too weak or too remote from the depositional flow-boundary zone to interrupt processes there and thus leave a depositional record.

Interaction with soft lake-bed substrate

Loading-related liquefaction widely affected the lake-bed sediments beneath the Pavey Arc ignimbrite. The basal contact is highly uneven in many places and the lacustrine sandstone and siltstone immediately beneath it are convoluted, partially homogenized (Figs. 4 and 10) and locally occur as sheets injected upwards into the ignimbrite. At deeper levels, and also above the Pavey Ark unit, bedding is relatively undisturbed. Caldera faulting probably contributed to the effects of loading, via seismic shaking and slumping.

Soft-state loading and injection of sediment evidently occurred at various times during aggradation of the ignimbrite. At one location (log 6 in Fig. 10a), the lowest few metres of the breccia foundered into and were penetrated by homogenized underlying sediments (Fig. 13a). This event must have occurred early during breccia aggradation, because the basal irregularities do not affect diffuse planar layers within the breccia a few metres above the base. The current must have planed-off and re-entrained those basal deposits that were extruded upwards during the early deformation, while ignimbrite breccia deposition in general continued. In contrast, at Cam Crag (NY 2618 1115), a sedimentary dyke penetrates 28 m upwards into the Pavey Ark ignimbrite. The dyke shows no deformation (Fig. 13b) and records injection after deposition of at least 28 m of breccia.

Caldera subsidence during the eruption

Volcanotectonic subsidence accompanied the Pavey Arc explosive eruption, affecting areas as much as 12 km from the inferred vent location. Volcanotectonic fault movement is shown by marked thickness changes of the ignimbrite and by localised intense soft-state deformation, and it demonstrably occurred during emplacement of the ignimbrite and associated co-ignimbrite ash.

Before the Pavey Arc eruption, the north-trending Troughton Beck Fault (Fig. 2 centre) had been active with downthrow to the east, but by the time of the eruption the topography this fault produced had mostly been infilled by lake sediments (Kneller and McConnell 1993). The ignimbrite breccia (lithofacies mScBr and mTScBr) shows a marked reduction in grain-size and an increase in the proportion of matrix westwards across the fault, which indicate that there was sufficient topography during breccia emplacement to impede the current (partial blocking) and thus enhance the deposition of large blocks east of the fault. The ignimbrite thins dramatically from 125 m east of the fault to 40 m just 350 m to the west (Figs. 10a and 11). This thickness change cannot simply reflect lake-floor topography that existed before the current incursion, because this would imply a slope of ≥12°, too steep for the water-saturated sands and silts of the contemporary lake-bed to have remained stable. Rather, the field relations indicate that rapid lake-floor faulting accompanied deposition of the ignimbrite, producing topography beneath the current sufficient to affect the breccia sedimentation and cause infilling that more or less kept pace with the subsidence. The large and rapid displacement on this fault involved some 65 m of subsidence *during* the Pavey Ark eruption and, taken together with other indications of contemporary subsidence, is evidence for an increment of caldera collapse linked to the eruption. The fault lies ~7 km west of the inferred vent location.

Although some aspects of the basin-floor topography and caldera subsidence are well shown by the restoration of the top of the breccia and lapilli-tuff to horizontal (Fig. 11), this restoration produces, as an artefact, a 'mound' of massive tuff ($mT_{(n)}$) and very fine tuff (vfmT) >40 m thick in north-central areas of the caldera (Cam Crag and Sergeant's Crag; logs 19 and 20 in Figs. 10b and 11). A subaqueous pile >40 m high of uncompacted, unconsolidated ash is inconceivable; such a deposit would be fluid and spread gravitationally to near-horizontal. We deduce that for the top of the Pavey Ark unit to have been near-horizontal by the end of its sedimentation, it must have accumulated within a lake-floor depression that developed *at a late stage during* its aggradation. Thus, although the uppermost extensive spatter-rich (entrachron) layer must have sloped fairly uniformly westwards when it was deposited, parts of it (e.g. at Cam Crag and Rossett Gill; Figs. 10a, b and 11) must have subsided rapidly several tens of metres soon afterwards, while the fine-ash top was still accumulating. This syn-eruptive caldera subsidence affected an area up to 12 km from the inferred source (e.g. log 3 on Figs. 10a and 11).

Volcanotectonic activity mobilized the entire thickness of the Pavey Ark unit near the Blea Tarn Faults (Fig. 2 top right), in the north of the caldera lake, ~7 km from the inferred vent. In the vicinity of Standing Crag (Fig. 10b), the lower contact of the ignimbrite is extremely uneven; locally, the massive breccia (mScBr) is truncated at steep contacts against disrupted substrate (Fig. 14). The uneven lower contact is a slide surface, with steep lateral ramps, upon which the entire thickness of the ignimbrite moved. Also in this area, the ignimbrite thins from ≥60 to ≤30 m (logs 24 and 22, respectively, Fig. 10b) across a distance of 300 m (Figs. 11 and 14). Where the ignimbrite is thickest, it is conformably overlain by sandstone and siltstone, as is the case widely across the basin, but farther west these beds lie upon a discordant slide surface that cuts westwards down through the upper part of the ignimbrite (Fig. 14). This geometry indicates that whole-

sale sliding of the ignimbrite was accompanied by localised slumping of upper parts.

Seven hundred metres farther north, at Bell Crags (NY 299 146), the ignimbrite is chaotically disrupted. The lower, block-rich part has numerous steep internal contacts (e.g. 4–8 m on log 25, Fig. 10b) and it encloses slabs, up to 2 m thick and 8 m long, of the upper, fine-grained tuff ($mT_{(n)}$; 10–13 m on log 25, Fig. 10b). This part is overlain by a complex succession of interleaved lapilli-tuff, medium tuff, and discontinuous bodies of breccia; at several localities, sections of the normal-graded tuff ($mT_{(n)}$) show repetition across slide surfaces. This soft-state disruption affects the underlying substrate, and the whole package here is interpreted as a slumped mass. Notionally, at least, the slumped mass is the down-flow counterpart to the locality at Standing Crag, where the whole deposit was shifted and part of the sequence is missing. The deformation occurred during or very soon after the Pavey Ark eruption, because no post-ignimbrite lacustrine sediments were involved in the slumping and slide-repetition.

Although sliding and slumping on a wet substrate can initiate on slopes as slight as 1–2° (e.g. Lewis 1971), the ignimbrite at Standing Crag must have been elevated by at least some 30–50 m relative to the deposit 700 m farther north, at Bell Crags, to facilitate deep detachment (tens of metres down) as well as imbricate stacking of the slumped material where it stopped. The relative elevation and slumping of ignimbrite were probably caused by movements on the northwest-trending Blea Tarn Faults, which lie between the two localities of interest (Fig. 10b inset). The fault zone had been active previously during the climactic caldera-forming eruption at Scafell caldera (Branney and Kokelaar 1994) and also during caldera-lake sedimentation, when it influenced sediment transport pathways (Kneller and McConnell 1993). We infer that during the Pavey Arc eruption it was reactivated again, with downthrow towards north-east. As with the Troughton Beck Fault described above, substantial lake-floor topography prior to the Pavey Ark eruption could not have been maintained in wet sediments, and the large scale and timing of the disturbance suggest that the faulting was related to the eruptive withdrawal of magma.

Similar soft-state slumping also affected the ignimbrite some 9 km west of source at Bowfell (near log 7, Fig. 10a), where downthrow of some 20 m towards the south occurred on a steep, listric surface marked by disrupted tuffs. Here again, overlying strata were not involved and syn-eruptive volcanotectonic subsidence is invoked.

In summary, there are several indications of substantial and widespread volcanotectonic faulting within the caldera lake during accumulation of the Pavey Arc unit. At distances of 7–12 km from the inferred vent, displacement across single faults amounted to at least 65 m and overall subsidence of the lake floor was probably greater. Near to the vent, in the south-east, caldera subsidence is likely to have been of the order of 500 m. Here, Pavey Ark breccia exceeds 500 m in thickness (Fig. 2) and there is no evidence for construction of any steep subaerial cone; we found no evidence of local reworking or alluvial facies that would indicate presence of such an edifice.

Behaviour of the pyroclastic density current in the lake

The Pavey Ark ignimbrite and co-ignimbrite tuff show what might have happened within modern flooded calderas during major eruptions, for example at Aira, Campi Flegrei, Krakatau, Santorini and Taal caldera volcanoes, where the intracaldera deposits are poorly known. We interpret the ignimbrite as the deposit of a high-mass-flux pyroclastic density current that entered Scafell caldera lake from a major explosive eruption on its eastern side (Figs. 15 and 16). Even where the ignimbrite is >120 m thick, it shows no evidence of shallowing to within wave-base; there are no wave-related sedimentary structures within its upper part or in the immediately overlying lacustrine strata, which accumulated more slowly.

We have no data on the exact configuration or conditions of entry of the Pavey Ark current into the lake (e.g. vent level relative to the water surface, slope angle, current thickness, density profile). From the fine-grained, water-settled top, we know that in the study area the current was subaqueous. The general absence of tractional stratification within the lacustrine ignimbrite indicates that the pyroclastic current was granular-fluid-based. Much of the lacustrine underflow must have ingested lake water, around its leading edges as it spread across the lake floor, and along upper mixing zones throughout the current duration (e.g. Simpson 1997, Ch. 11). However, the spatter within the massive breccias (mAg, mScBr) shows no signs of aqueous chilling, suggesting that at least proximally the lowermost part of the current remained a gaseous dispersion during several kilometres of subaqueous runout (Fig. 16). The gaseous dispersion must have been denser than any surrounding aqueous particulate dispersion, certainly denser than ~10^3 kg m^{-3}; we envisage a basal solids concentration ≥40–45 vol.% with poor sorting (low voidage) and with the gaseous phase heavily charged with ash (dusty gas). This condition would limit turbulent mixing. Retention of gas in the underflow also implies that the mass-flux of the current and the thickness of its basal gaseous part were sufficiently large to preclude complete admixture of water for a significant duration, long enough for runout of a few kilometres. Vigorous upward displacement of interstitial fluid (gas-plus-fines) from the concentrated dispersion during rapid deposition of coarse particles would have hindered downward penetration of liquid water

(fluid-escape-dominated flow-boundary zone of Branney and Kokelaar 2002, pp 57–60).

Sustained exclusion of liquid water from within a subaqueous hot particulate current has been invoked elsewhere, to account for fluidal spatter in basaltic submarine deposits (Kokelaar 1986; Head and Wilson 2003) and for submarine welded ignimbrite in the geological record, e.g. distal Capel Curig Volcanic Formation (Howells et al. 1985), Vandever Mountain Tuff (Kokelaar and Busby 1992), and the Pitts Head Tuff (Kokelaar and Königer 2000). Entrance of pyroclastic density currents into water from above has been simulated in experiments (McLeod et al. 1999; Freundt 2003), which show that dense gaseous granular flows can persist under water (albeit briefly in the experiments), before becoming entirely water-saturated or before they loft off the basin floor. Experiments involving rapid granular flows of hot (>200°C) samples of ignimbrite that enter water on a 26° slope indicate that dispersions slightly less dense than water may penetrate the water surface and flow just beneath it, mixing with the water, causing explosions, and producing sinking plumes of ash (Freundt 2003). Such behaviour of a part of the Pavey Ark current would not register clearly in the ignimbrite, but would have contributed to the settling suspension (Fig. 16).

Segregation during proximal deposition

The pyroclastic current that deposited the ~120 m-thick proximal breccias within the caldera at Pavey Arc behaved in a fashion similar to proximal outflow currents associated with caldera-forming eruptions elsewhere. The general proximal-to-distal decrease in the maximum clast size reflects decreasing (depletive) current competence, probably accompanied by depletive current capacity (e.g. Kneller and Branney 1995; Branney and Kokelaar 2002).

Kneller and McCaffrey (2003) have proposed that deposition resulting from depletive capacity simultaneously involves all grain sizes contained within the current, producing poorly sorted deposits. This is not straightforwardly the case with granular-fluid-based currents, such as the Pavey Arc current, because particle segregation accompanies the rapid deposition of large clasts, which displace interstitial fluid upwards. The upward flow of displaced fluid selectively hinders deposition of smaller clasts according to their size and density, and elutriates the ash and pumice, substantial proportions of which overpass to more distal locations. As with subaerial proximal ignimbrite breccia (e.g. Druitt and Sparks 1982; Druitt and Bacon 1986), the proximal Pavey Arc ignimbrite breccia does contain ash and pumice lapilli, but it contains far less than was in the original parent underflow. Evidence for this is that the breccia passes gradationally into voluminous fines-rich and eutaxitic lithofacies, both down-current and up-section. The variable abundance of the fine-tuff matrix within the breccia indicates that the elutriation flux varied, presumably as a result of changing (unsteady) rates of deposition. Broadly, the least matrix occurs in the coarsest breccias, which suggests that the most effective expulsion of interstitial fluid and ash was associated with deposition of blocks with the largest settling velocities. In contrast, where the depositing clasts were smaller (smaller blocks and lapilli), with lower settling velocities, there was less vigorous expulsion of fluid-plus-fines, so that the finer breccias and lapilli-tuffs contain more abundant fine-tuff matrix and fiamme.

Current entrapment and the thick co-ignimbrite ash

The finer-grained and more pumiceous constituents in the lacustrine underflow were preferentially carried down-current to be deposited more distally or to become suspended in the water column. Had the body of water been unconfined, most of the ash in the water column would have been deposited elsewhere and the fine-ash layer at the top of the ignimbrite would be much thinner. This is the case, for example, with the submarine outflow ignimbrite from Snowdon caldera (Lower Rhyolitic Tuff; Howells et al. 1986), which has only a 30 cm-thick layer of very fine tuff at its top. We ascribe the great thickness of the fine tuff within the upper part of the Pavey Arc unit (lithofacies $mT_{(n)}$ and vfmT; ≤55 m thick; Fig. 10) to entrapment of the suspension from the current within a confined (caldera lake) basin. Anomalously thick (tens of metres) fine tuffs have previously been recorded at the top of *submarine* intracaldera ignimbrites, where they are similarly attributed to entrapment of aqueous co-ignimbrite suspensions (Cader Rhwydog Tuff, Kokelaar et al. 1985; Vandever Mountain Tuff, Kokelaar and Busby 1992). Similarly, anomalously thick silt divisions at the top of some turbidites have been ascribed to entrapment of sediment gravity currents in closed marine basins (e.g. Pickering and Hiscott 1985; Ricci-Lucci and Valamori 1980; Haughton 1994), although these deposits are thinner and more laterally extensive than the intracaldera deposits.

Although considerable amounts of fine ash were deposited from the current, we infer that substantial amounts of ash mixed with lake water, around advancing edges of the current and along upper turbulent mixing zones (Fig. 16), forming a lacustrine ash plume that probably occupied most of the water column. This plume may be regarded as the subaqueous equivalent of atmospheric co-ignimbrite or phoenix plumes that loft above subaerial pyroclastic density currents and can account for up to 50% of the subaerial current mass (Sparks and Walker 1977; Sparks et al. 1997). In the Pavey Ark case, about 25% of the preserved unit was

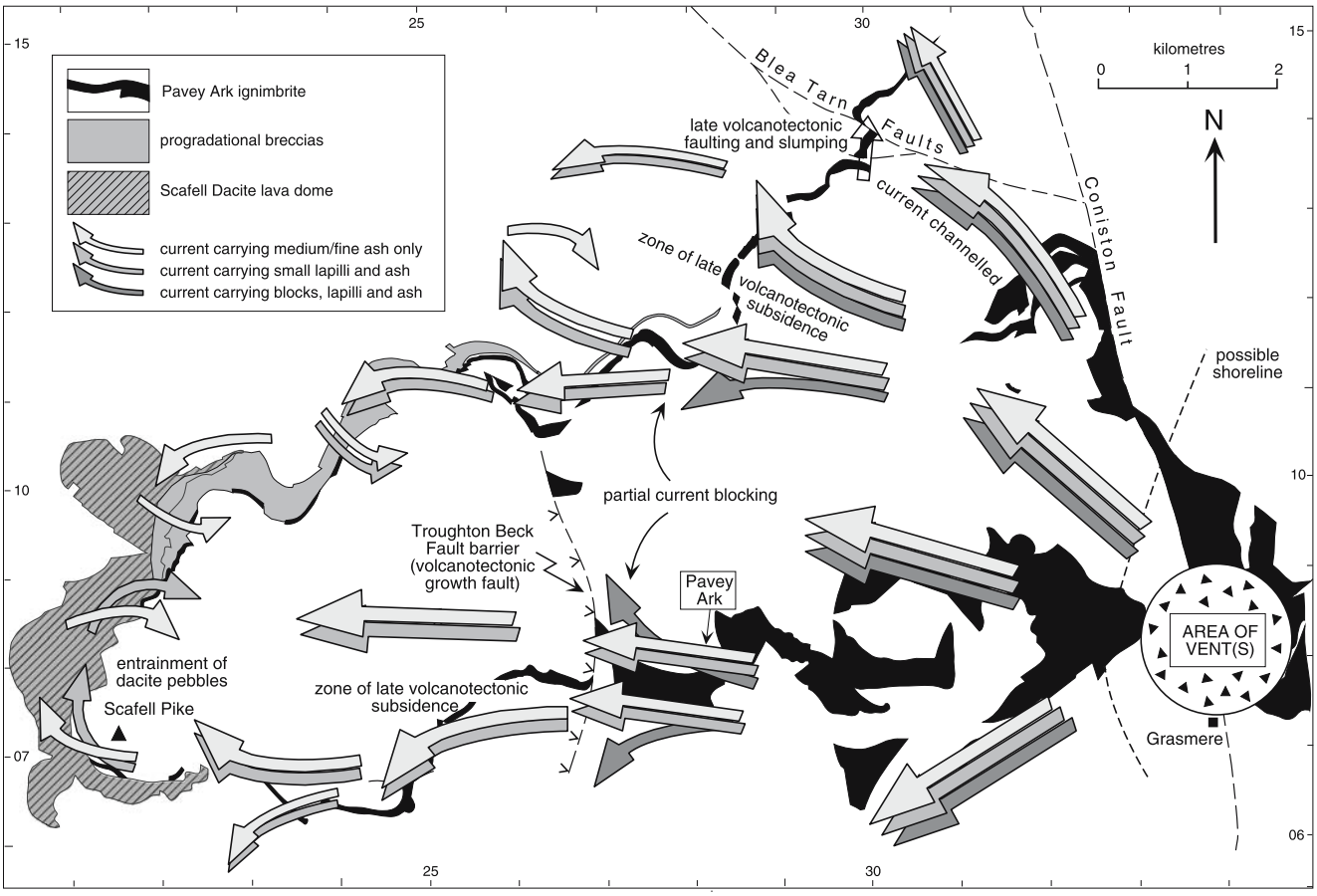

Fig. 15 Overall model describing the subaqueous behaviour of the Pavey Ark pyroclastic density current, depicting source vent(s), current direction and stratification in terms of transported load, active (volcanotectonic) faults, and lake-floor topographic obstacles

formed from the lacustrine ash suspension (0.2–0.25 km^3 of the 1 km^3; Table 1), and we infer that the suspension must have been moderately concentrated; to form the fine-grained top from a *dilute* aqueous suspension (solids ≤0.1% of volume) would have required a very deep water column with extraordinarily steady settling sustained for a very long time.

The uppermost layer of eutaxitic lapillistone or eutaxitic lapilli-tuff (empL, empLT), which records the final sinking of water-logged pumice lapilli, is thickest in the west (locally up to 7 m). It is possible that wind influenced the lake-surface distribution of the floating lapilli. The absence of the fine-grained lithofacies (mT$_{(n)}$ and vfmT) in the south-eastern, proximal region of the ignimbrite may be due to non-deposition or erosion; a post-eruption inflow of stream water into the lake from the south-east may have prevented fine ash from remaining there.

Nature of the Pavey Ark eruption

There is robust evidence that the Pavey Ark eruption involved 5 km^3 of magma, and there are indications that the actual volume was considerably larger. We do not know the total volcanotectonic subsidence that accompanied the eruption, but an erupted volume >>5 km^3 would be consistent with the ≥65 km^2 area of syn-eruptive subsidence. This area, broadly reflecting the existence of a large contemporary magma chamber, is much larger than (1) the <5 km^2 that subsided during the 5 km^3 DRE climactic eruption of Mount Pinatubo in 1991 (Campita et al. 1996; Scott et al. 1996; Wolfe and Hoblitt 1996), (2) the ~10 km^2 that subsided during the 13±3 km^3 DRE eruption of Novarupta in 1912 (Fierstein and Hildreth 1992), (3) the ~28 km^2 that subsided during the 50 km^3 DRE eruption of Tambora in 1815 (Sigurdsson and Carey 1989), and (4) the ~50 km^2 that subsided during the >12 km^3 DRE eruption of Krakatau in 1883 (Mandeville et al. 1996). The exposed Pavey Ark deposit (Fig. 2) may represent only the north-west, *intracaldera*, sector of a more symmetrical distribution from the eruptive source, involving an extensive subaerial outflow sheet. A component of the Pavey Ark current may have crossed the water and traversed land beyond, as during the Campanian eruption in the north of the Bay of Naples (Barberi et al. 1978; Fisher et al. 1993; Rosi et al. 1996) and during the

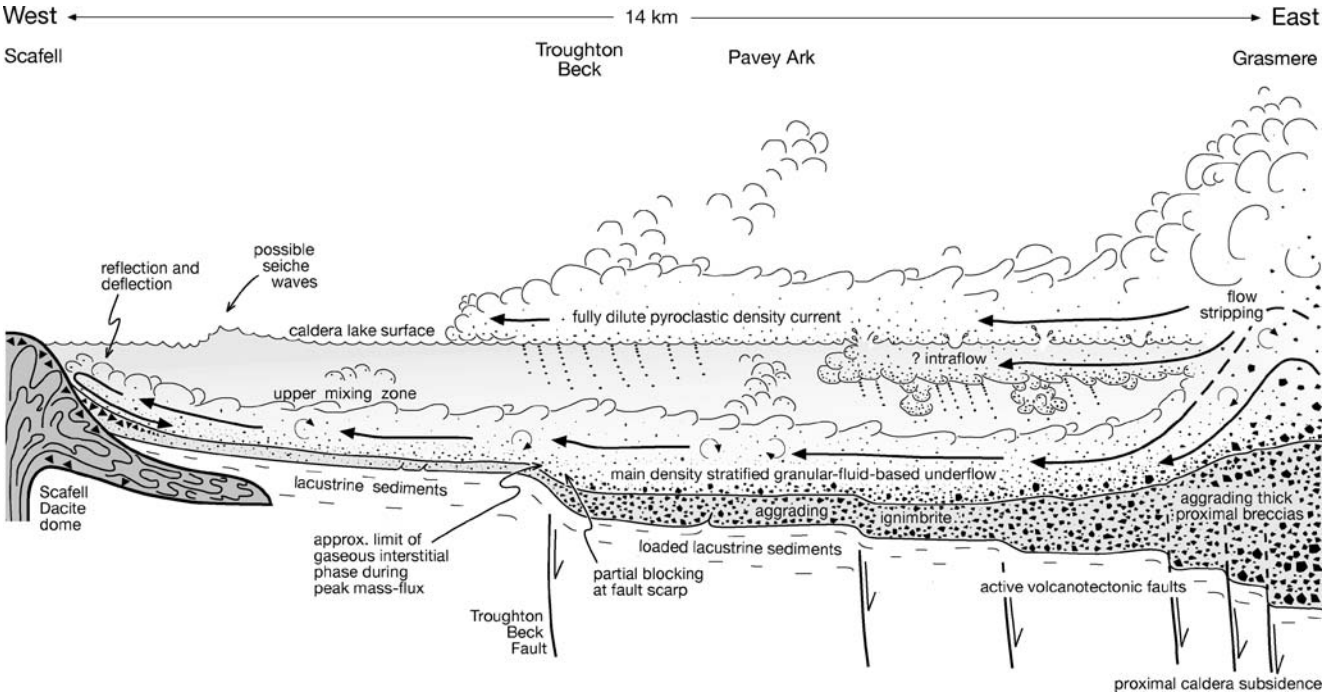

Fig. 16 Model of Pavey Ark pyroclastic density current behaviour in cross-section. The main underflow selectively deposited breccia in the proximal area, where aggradation was strongly influenced by contemporaneous caldera subsidence, while finer pyroclasts overpassed to be deposited in medial to distal areas or to mix into the overlying water column. A stripped fully dilute pyroclastic density current travelled across the lake surface, depositing particles into the water column, while an intraflow formed just beneath the lake surface, where there was vigorous steam explosivity and additional settling into the water (Freundt 2003); one or more seiche waves propagated away from the site(s) of entry of the current into the lake. The depictions of relative east-to-west travel distances of the seiche wave (s), flows above and below the lake surface, and the main underflow, are for cartographic convenience; the stripped fully dilute current may well have crossed the lake long before the main underflow interacted with the Scafell Dacite lava dome (far west), by which time also much of the water column would have been substantially choked with ash and the various phenomena and their physical processes would have become entangled

1883 eruption at Krakatau, when a hot, fully dilute current travelled over the sea for several tens of kilometres to cause damage and deposit ignimbrite on mainland Sumatra (Camus and Vincent 1983; Sigurdsson et al. 1991; Carey et al. 1996; Mandeville et al. 1996). There may also have been a significant volume of (unrecognised) fallout. From the extent of the volcanotectonic subsidence, we favour the interpretation that the Pavey Arc lacustrine ignimbrite represents only a small part of a much larger pyroclastic deposit (e.g. ≥VEI 6).

By comparison with historical caldera-forming eruptions, the Pavey Arc eruption and associated pyroclastic density current probably lasted for at least a few hours. In 1991 Mount Pinatubo erupted ~5 km^3 of (dense) magma in ~8 h (Scott et al. 1996; Wolfe and Hoblitt 1996), in 1912 Novarupta erupted 13±3 km^3 of magma within 3 days, with episodes of enhanced rates (Fierstein and Hildreth 1992), and in 1815 Tambora produced several tens of cubic kilometres of ignimbrite within 2 or 3 days (Self et al. 1984; Sigurdsson and Carey 1989).

Regarding the course and mechanism(s) of the explosive activity, the caldera-lake succession does not clearly record any immediate precursory activity or aftermath landscape response. A Plinian precursor cannot be discounted, however, because any fallout pumice may have floated. There is evidence for surging of the Pavey Ark current, which facilitated enhanced transport of spatter, and then waning, but otherwise there is nothing to indicate any change in material supply.

Although the scoria, fiamme (collapsed pumice) and vesicle-wall shards indicate magmatic explosivity, it is probable that magma fragmentation also involved external water. The blocky and angular shards associated with poorly vesicular juvenile clasts can be taken to indicate magma-water interaction (e.g. Heiken and Wohletz 1985, 1991), either prior to vesiculation, or with batches of magma that were relatively gas-poor (e.g. Houghton et al. 2000). In common with many large-magnitude explosive eruptions at flooded calderas (e.g. at Campi Flegrei, Santorini and Taal), it is uncertain whether the Pavey Ark eruption was subaqueous and emergent (breaking the water surface), or fully subaerial, and unclear how water may have accessed the magma. The observation that spatter is commonly ejected along with scoria or pumice and ash during large eruptions at flooded calderas may have some bearing on this problem. The occurrence of spatter at numerous levels in the Pavey Ark

ignimbrite implies persistent or recurrent eruption of relatively gas-poor magma along with the gas-rich magma. This coincidence may arise where a magma chamber has a volatile-rich cap and evacuation is so rapid as to tap deeper, volatile-poor levels as well (e.g. Spera 1984). However, the lithic fragments embedded within the spatter suggest another mechanism.

The juvenile andesitic scoria and spatter within the proximal breccia of the Pavey Arc ignimbrite closely resemble basaltic to dacitic spatter in proximal ignimbrite agglomerates and breccias at Campi Flegrei (Perrotta and Scarpati 1994; Rosi et al. 1996), Santorini (Druitt and Sparks 1982; Druitt 1985; Druitt et al. 1989; Mellors and Sparks 1991), Taal (Branney and Kokelaar 2002), Vanuatu (Robin et al. 1994; Allen 2005) and Vulsini (Marsella et al. 1987; Palladino and Simei 2004); the close resemblance suggests a common origin. Angular lithic lapilli within the poorly vesicular spatter on Santorini have been interpreted as recording hydromagmatic explosivity, when water entered a deep crater containing the relatively degassed magma (Mellors and Sparks 1991). The angular lithic lapilli are remarkably similar to those commonly found in another setting, within large, dense magma clasts (e.g. cauliflower bombs) in phreatomagmatic tuff-rings (Fisher and Schmincke 1984). In the Pavey Ark case, the only evidence for involvement of external water in the eruption is in the relatively high proportions of blocky, angular shards that accompany low-vesicularity juvenile clasts. In contrast to the proximal ignimbrite scoria-agglomerates at Santorini and elsewhere, the juvenile clasts at Pavey Ark appear to lack distinct surficial cracking due to cooling-contraction around a hot-deforming interior and hence do not preserve evidence for direct contact with liquid water. We hypothesize that the initial withdrawal of magma could have resulted in pressure reduction sufficient to cause either conduit collapse with ingress of lake water, or explosive expansion and disruption of a sub-lacustrine groundwater-hydrothermal system adjacent to the evacuating chamber, or both. Disruption of a hydrothermal system could force out gas-poor magma along with gas-rich magma, while at the same time admixing the small lithic fragments (e.g. Mellors and Sparks 1991). In the Pavey Arc spatter, because of pervasive low-grade metamorphic alteration, we cannot distinguish any hydrothermal alteration of the included lithic clasts, but this need not have been substantial at the time of the eruption. Whatever the mechanism, it appears to have been sustained for most of the duration of the current (a few hours), because there is no record in the deposit of a temporal change from magmatic to phreatomagmatic explosivity, e.g. abrupt change in grainsize or shard shape with height, and there is no evidence (such as an extensive lithic breccia horizon) for an abrupt collapse that might have triggered the sudden ingress of water (cf. Palladino and Simei 2004). Caldera subsidence seems to have occurred throughout ignimbrite deposition. The lack of any dramatic change in the nature of the (recorded) eruption favours a mechanism involving magmatic explosivity persistently enhanced by steam from the disruption of a hydrothermal system. The Pavey Arc case, together with the general association of flooded calderas with ignimbrites containing fluidal-shaped juvenile scoria and spatter, suggests that the caldera lake plays a role in providing water to the sub-lacustrine aquifer-hydrothermal system during the caldera-forming eruption. Straightforward mixing of erupting magma with a standing body of water is not indicated.

Acknowledgements We gratefully acknowledge NERC Grant F60/G2/31 awarded (to PK) to map the Scafell caldera, and funding via a Shell PhD Scholarship Award (to PR). We greatly benefited from discussions with Ben Kneller and Brian McConnell, who mapped the caldera with us. We are indebted to Kay Lancaster for her expert cartographic assistance and infinite patience, and to Helen Kokelaar for compiling the reference list. Thorough and thoughtful reviews by Malcolm Howells, Vern Manville and Jocelyn McPhie substantially improved the style and content of the paper. We also thank Eric Johnson and Tony Reedman for insights regarding the geology east of Pavey Ark.

References

Alexander J, Morris S (1994) Observations on experimental, non-channelized, high-concentration turbidity currents and variations in deposits around obstacles. J Sediment Petrol A64:899–909

Allen SR (2005) Complex spatter- and pumice-rich pyroclastic deposits from an andesitic caldera-forming eruption: the Siwi pyroclastic sequence, Tanna, Vanuatu. Bull Volcanol 67:27–41

Arnott RWC, Hand BM (1989) Bedforms, primary structures and grain fabric in the presence of suspended sediment rain. J Sediment Petrol 59:1062–1069

Barberi F, Innocenti F, Lirer L, Munno R, Pescatore T, Santacroce R (1978) The Campanian ignimbrite: a major prehistoric eruption in the Neapolitan area. Bull Volcanol 41:10–31

Branney MJ (1988) The subaerial setting of the Ordovician Borrowdale Volcanic Group, English Lake District. J Geol Soc (Lond) 145:887–890

Branney MJ, Kokelaar BP (1992) A reappraisal of ignimbrite emplacement: progressive aggradation and changes from particulate to non-particulate flow during emplacement of high-grade ignimbrite. Bull Volcanol 54:504–520

Branney MJ, Kokelaar BP (1994) Rheomorphism and soft-state deformation of tuffs induced by volcanotectonic faulting at a piecemeal caldera, English Lake District. Geol Soc Amer Bull 96:507–530

Branney MJ, Kokelaar P (2002) Pyroclastic density currents and sedimentation of ignimbrites. Geol Soc London (Mem) 27:1–138

Branney MJ, Soper NJ (1988) Ordovician volcano-tectonics in the English Lake District. J Geol Soc (Lond) 145:367–376

Branney MJ, Sparks RSJ (1990) Fiamme formed by diagenesis and burial-compaction in soils and subaqueous sediments. J Geol Soc (Lond) 147:919–922

British Geological Survey (1996) Ambleside. England and Wales Sheet 38. Solid Geology 1:50 000. Keyworth, Nottingham, British Geological Survey

Brown RJ (2001) The eruption histories and depositional mechanisms of the Poris ignimbrite of Tenerife and the Glaramara tuff of the English Lake District. PhD thesis, University of Leicester, England

Brown RJ, Branney MJ (2004) Bypassing and diachronous deposition from density currents: evidence from a giant regressive bedform in the Poris ignimbrite, Tenerife. Geology 32:445–448

Burgisser A, Bergantz GW (2002) Reconciling pyroclastic flow and surge: the multiphase physics of pyroclastic density currents. Earth Planet Sci Lett 202:405–418

Campita NR, Daag AS, Newhall CG, Rowe GL, Solidum RU (1996) Evolution of a small crater lake at Mount Pinatubo. In: Newhall CG, Punongbayan RS (eds) Fire and mud—eruptions and lahars of Mount Pinatubo, Philippines. Philippine Institute of Volcanology and Seismology, Quezon City and University of Washington Press, Seattle, pp 435–442

Camus G, Vincent PM (1983) Discussion of a new hypothesis for the Krakatau volcanic eruption in 1883. J Volcanol Geotherm Res 19:167–173

Carey SN (1997) Influence of convective sedimentation on the formation of widespread tephra fall layers in the deep sea. Geology 25:839–842

Carey SN, Sigurdsson H (1980) The Roseau Ash: deep-sea tephra deposits from a major eruption on Dominica, Lesser Antilles Arc. J Volcanol Geotherm Res 7:67–86

Carey SN, Sigurdsson H, Sparks RSJ (1988) Experimental studies of particle-laden plumes. J Geophys Res 93:1514–1528

Carey SN, Sigurdsson H, Mandeville C, Bronto S (1996) Pyroclastic surges and flows over water: an example from the 1883 Krakatau eruption. Bull Volcanol 57:493–511

Channell JET, McCabe C (1992) Palaeomagnetic data form the Borrowdale Volcanic Group: volcano-tectonics and Late Ordovician palaeolatitudes. J Geol Soc (Lond) 149:881–888

Clavero JE, Moreno H (1994) Ignimbritas Licán y Pucón: evidencias de erupciones explosivas andesítico-basálticas postglaciales del volcán Villarica, Andes del Sur, 39°25′S. (Congreso Geológico Chileno 7, Concepción, Chile) Actas 1:250–254

Cole RB, DeCelles PG (1991) Subaerial to submarine transitions in early Miocene pyroclastic flow deposits, southern San Joaquin basin, California. Geol Soc Amer Bull 103:221–235

Druitt TH (1985) Vent evolution and lag breccia formation during the Cape Riva eruption of Santorini, Greece. J Geol 93:439–454

Druitt TH (1995) Settling behaviour of concentrated, poorly sorted dispersion and some volcanological applications. J Volcanol Geotherm Res 65:27–39

Druitt TH, Bacon CR (1986) Lithic breccia and ignimbrite erupted during the collapse of Crater Lake Caldera, Oregon. J Volcanol Geotherm Res 29:1–32

Druitt TH, Sparks RSJ (1982) A proximal ignimbrite breccia facies on Santorini volcano, Greece. J Volcanol Geotherm Res 13:147–171

Druitt TH, Mellors RA, Pyle DM, Sparks RSJ (1989) Explosive volcanism on Santorini, Greece. Geol Mag 126:95–126

Edwards DA, Leeder MR, Best JL, Pantin HM (1994) On experimental reflected density currents and the interpretation of certain turbidites. Sedimentology 41:437–461

Fierstein J, Hildreth W (1992) The Plinian eruptions of 1912 at Novarupta, Katmai National Park, Alaska. Bull Volcanol 54:646–684

Fisher RV (1990) Transport and deposition of a pyroclastic surge across an area of high relief—the 18 May 1980 eruption of Mount St. Helens, Washington. Geol Soc Amer Bull 92:938–954

Fisher RV, Schmincke H-U (1984) Pyroclastic rocks. Springer, Berlin Heidelberg New York

Fisher RV, Orsi G, Ort M, Heiken G (1993) Mobility of a large volume pyroclastic flow—emplacement of the Campanian ignimbrite, Italy. J Volcanol Geotherm Res 56:205–220

Fiske RS (1963) Subaqueous pyroclastic flows in the Ohanapecosh Formation, Washington. Geol Soc Amer Bull 74:391–406

Fiske RS, Matsuda T (1964) Submarine equivalents of ash flows in the Tokiwa Formation, Japan. Am J Sci 262:76–106

Freundt A (2003) Entrance of hot pyroclastic flows into the sea: experimental observations. Bull Volcanol 65:144–164

Haughton PDW (1994) Deposits of deflected and ponded turbidity currents, Sorbas basin, southeast Spain. J Sediment Res 44:233–246

Head JW, Wilson L (2003) Deep submarine pyroclastic eruptions: theory and predicted landforms and deposits. J Volcanol Geotherm Res 121:155–193

Heiken G, Wohletz KH (1985) Volcanic ash. University of California Press, Berkeley, CA

Heiken G, Wohletz K (1991) Fragmentation processes in explosive volcanic eruptions. In: Fisher RV, Smith GA (eds) Sedimentation in volcanic settings. SEPM (Special Publication), pp 19–26

Houghton BF, Wilson CJN, Smith RT, Gilbert JS (2000) Phreatoplinian eruptions. In: Sigurdsson H, Houghton B, Mcnutt S, Rymer H, Stix J (eds) Encyclopedia of volcanoes. Academic, San Diego, CA, pp 513–525

Howells MF, Campbell SDG, Reedman AJ (1985) Isolated pods of subaqueous welded ash-flow tuff: a distal facies of the Capel Curig Volcanic formation (Ordovician), North Wales. Geol Mag 122:175–180

Howells MF, Reedman AJ, Campbell SDG (1986) The submarine eruption and emplacement of the lower Rhyolitic Tuff formation (Ordovician), N Wales. J Geol Soc (Lond) 143:411–423

Kneller BC, Branney MJ (1995) Sustained high-density turbidity currents and the deposition of thick massive sands. Sedimentology 42:607–616

Kneller BC, McCaffrey WD (2003) The interpretation of vertical sequences in turbidite beds: the influence of longitudinal flow structure. J Sediment Res 73:706–713

Kneller BC, McConnell BJ (1993) The Seathwaite Fell formation in the Central Fells. British Geological Survey Technical report WA/93/43

Kneller BC, Edwards DA, McCaffrey WD, Moore RM (1991) Oblique reflection of turbidity currents. Geology 19:250–252

Kneller BC, Kokelaar BP, Davis NC (1993) The lingmell formation. British Geological Survey Technical report WA/93/42

Kneller BC, Bennett SJ, McCaffrey WD (1997) Velocity and turbulence structure of gravity currents and internal solitary waves: potential sediment transport and formation of wave ripples in deep water. Sed Geol 112:235–250

Kokelaar BP (1986) Magma-water interactions in subaqueous and emergent basaltic volcanism. Bull Volcanol 48:275–289

Kokelaar BP (1992) Ordovician marine volcanic and sedimentary record of rifting and volcanotectonism: Snowdon, Wales, United Kingdom. Geol Soc Amer Bull 94:1433–1455

Kokelaar BP, Busby C (1992) Subaqueous explosive eruption and welding of pyroclastic deposits. Science 257:196–201

Kokelaar BP, Königer S (2000) Marine emplacement of welded ignimbrite: the Ordovician Pitts Head Tuff, North Wales. J Geol Soc (Lond) 157:517–536

Kokelaar BP, Bevins RE, Roach RA (1985) Submarine silicic volcanism and associated sedimentary and tectonic processes, Ramsey Island, SW Wales. J Geol Soc (Lond) 142:591–613

Lewis KB (1971) Slumping on a continental slope inclined at 1°–4°. Sedimentology 16:97–110

Loughlin SC, Calder ES, Clarke A, Cole PD, Luckett R, Mangan MT, Pyle DM, Sparks RSJ, Voight B, Watts RB (2002) Pyroclastic flows and surges generated by the 25 June 1997 dome collapse, Soufrière Hills Volcano, Montserrat. In: Druitt TH, Kokelaar BP (eds) The eruption of Soufrière Hills Volcano, Montserrat, from 1995 to 1999. Geol Soc London, Mem 21:191–209

Mandeville CW, Carey S, Sigurdsson H (1996) Sedimentology of the Krakatau 1883 submarine pyroclastic deposits. Bull Volcanol 57:512–529

Manville V, Wilson CJN (2004) Vertical density currents: a review of their potential role in the deposition and interpretation of deep-sea ash layers. J Geol Soc (Lond) 161:947–958

Marsella M, Palladino DM, Trigila R (1987) The Onano Pyroclastic Formation (Vulsini volcanoes): depositional features, distribution and eruptive mechanisms. Period Mineral 56:225–240

Mattox TN, Mangan MT (1997) Littoral hydrovolcanic explosions: a case study of lava-seawater interaction at Kilauea Volcano. J Volcanol Geotherm Res 75:1–17

McConnell BJ (1993) The lincomb tarns and Esk Pike formations. British Geological Survey Technical report, WA/93/45

McLeod P, Carey S, Sparks RSJ (1999) Behaviour of particle-laden flows into the ocean: experimental simulation and geological implications. Sedimentology 46:523–536

Mellors RA, Sparks RSJ (1991) Spatter-rich pyroclastic flow deposits on Santorini, Greece. Bull Volcanol 53:327–342

Millward D (2002) Early Palaeozoic magmatism in the English Lake District. Proc Yorks Geol Soc 54:65–93

Muck MT, Underwood MB (1990) Upslope flow of turbidity currents—a comparison among field observations, theory, and laboratory models. Geology 18:54–57

Nelson CH, Meyer AW, Thor D, Larsen M (1986) Crater Lake, Oregon: a restricted basin with base-of-slope aprons of non-channelized turbidites. Geology 14:238–241

Nelson CH, Bacon CR, Robinson SW, Adam DP, Bradbury JP, Barber JH, Schwartz D, Vagenas G (1994) The volcanic, sedimentologic, and paleolimnologic history of the Crater Lake caldera floor, Oregon: Evidence for small caldera evolution. Geol Soc Amer Bull 106:684–704

Palladino DM, Simei S (2004) Eruptive dynamics and caldera collapse during the Onano eruption, Vulsini, Italy. Bull Volcanol 67:423–440

Pantin HM, Leeder MR (1987) Reverse flow in turbidity currents: the role of internal solitions. Sedimentology 34:1143–1155

Perrotta A, Scarpati C (1994) The dynamics of the Breccia Museo eruption (Campi Flegrei, Italy) and the significance of spatter clasts associated with lithic breccias. J Volcanol Geotherm Res 59:335–355

Pickering KT, Hiscott RN (1985) Contained (reflected) turbidity currents from the Mid-Ordovician Cloridorme formation, Quebec, Canada: an alternative to the anti-dune hypothesis. Sedimentology 32:373–394

Piper DJW, Normark WR (1983) Turbidite depositional patterns and flow characteristics, Navy Submarine Fan, California Borderland. Sedimentology 30:681–694

Piper JDA, Stephen JC, Branney MJ (1997) Palaeomagnetism of the Borrowdale and Eycott Volcanic Groups, English Lake District: primary and secondary magnetisation during a single upper Ordovician polarity chron. Geol Mag 134:481–506

Raine P (1998) Sedimentary processes and depositional environments in caldera lakes: Scafell (UK) and La Primavera (Mexico) calderas. PhD thesis, University of Liverpool, England

Ricci-Lucci F, Valamori E (1980) Basinwide turbidites in a Miocene oversupplied deep sea plain: a geometric analysis. Sedimentology 27:241–270

Robin C, Eissen JP, Monzier M (1994) Ignimbrites of basaltic andesite and andesite compositions from Tanna, New Hebrides arc. Bull Volcanol 56:10–22

Rosi M, Vezzoli L, Aleotti P, De Censi M (1996) Interaction between caldera collapse and eruptive dynamics during the Campanian ignimbrite eruption, Phlegraean Fields, Italy. Bull Volcanol 57:541–554

Scott WE, Hoblitt RP, Torres RC, Self S, Martinez ML, Nillos TJ (1996) Pyroclastic flows of the June 15, 1991, climatic eruption of Mount Pinatubo. In: Newhall CG, Punongbayan S (eds) Fire and mud—eruptions and lahars of Mount Pinatubo, Philippines. Philippine Institute of Volcanology and Seismology, Quezon City and University of Washington Press, Seattle, pp 545–570

Self S, Rampino MR, Newton MS, Wolff JA (1984) Volcanological study of the great Tambora eruption of 1815. Geology 12:65–663

Sigurdsson H, Carey S (1989) Plinian and co-ignimbrite tephra fall from the 1815 eruption of Tambora volcano. Bull Volcanol 51:243–270

Sigurdsson H, Carey S, Mandeville C, Bronto S (1991) Pyroclastic flows of the 1883 Krakatau eruption. Eos, Trans Am Geophys Union 72:377–392

Simpson JE (1997) Gravity currents in the environment and the laboratory, 2nd edn. Cambridge University Press, Cambridge

Sohn YK (1997) On traction-carpet sedimentation. J Sediment Res 67:502–509

Soper NJ, Webb BC, Woodcock NH (1987) Late Caledonian (Acadian) transpression in north-west England: timing, geometry and geotectonic significance. Proc Yorks Geol Soc 46:175–192

Sparks RSJ, Walker GPL (1977) The significance of vitric-enriched air-fall ashes associated with crystal-enriched ignimbrites. J Volcanol Geotherm Res 2:329–341

Sparks RSJ, Bursik MI, Carey SN, Gilbert JS, Glaze LS, Sigurdsson H, Woods AW (1997) Volcanic plumes. Wiley, Chichester

Spera FJ (1984) Some numerical experiments on the withdrawal of magma from crustal reservoirs. J Geophys Res 89:8222–8236

Thomas RME, Sparks RSJ (1992) Cooling of tephra during fallout from eruption columns. Bull Volcanol 54:542–553

Valentine GA (1987) Stratified flow in pyroclastic surges. Bull Volcanol 49:616–630

Valentine GA, Perry FV, WoldeGabriel G (2000) Field characteristics of deposits from spatter-rich pyroclastic density currents at Summer Coon volcano, Colorado. J Volcanol Geotherm Res 104:187–199

Vrolijk PJ, Southard JB (1998) Experiments on rapid deposition of sand from high-velocity flows. Geosci Can 24:45–54

Walker GPL (1985) Origin of coarse lithic breccias near ignimbrite source vents. J Volcanol Geotherm Res 25:157–171

White JDL, Houghton BF (2006) Primary volcaniclastic rocks. Geology 34:677–680

Whitham AG (1989) The behaviour of subaerially produced pyroclastic flows in a subaqueous environment: evidence from the Roseau eruption, Dominica, West Indies. Mar Geol 86:27–40

Whitham AG, Sparks RSJ (1986) Pumice. Bull Volcanol 48:209–223

Wolfe EW, Hoblitt RP (1996) Overview of the eruptions. In: Newhall CG, Punongbayan RS (eds) Fire and mud—eruptions and lahars of Mount Pinatubo, Philippines. Philippine Institute of Volcanology and Seismology, Quezon City and University of Washington Press, Seattle, pp 3–20

Woods AW, Bursik MI, Kurbatov AV (1998) The interaction of ash flows with ridges. Bull Volcanol 60:38–51

Wright JV, Mutti E (1981) The Dali Ash, Island of Rhodes, Greece: a problem in interpreting submarine volcanigenic sediments. Bull Volcanol 44:153–167

Wright JV, Walker GPL (1981) Eruption, transport and deposition of ignimbrite—a case-study from Mexico. J Volcanol Geotherm Res 9:111–131

Zalasiewicz JA, Hudson JD, Branney MJ, Böhm MF (1997) Emplacement of catastrophic submarine gravity flow deposit (Scheck Breccia, Austria): insights from matrix exceptionally preserved by early cementation (Abstract). In: 18th International Association of Sedimentologists Regional Meeting, Heidelberg, Germany, GAEA, Heidelberg 3:370